STUDY OF NATURAL CONVECTION HEAT TRANSFER IN AN ENCLOSURE WITH A HEAT GENERATING POROUS BED WITH WALL TEMPERATURE VARIATION

THESIS SUBMITTED IN PARTIAL FULFILMENT OF

THE REQUIREMENT FOR THE DEGREE OF

MASTER OF NUCLEAR ENGINEERING

BY

SUMAN MODAK

(UNIVERSITY REGISTRATION NO: 141081 OF 2017-18)

(EXAMINATION ROLL NO:M4NUE19004)

UNDER THE SUPERVISION OF

DR. SWARNENDU SEN

MECHANICAL ENGINEERING DEPARTMENT
JADAVPUR UNIVERSITY.
KOLKATA

SCHOOL OF NUCLEAR STUDIES & APPLICATION
FACULTY OF INTERDISCIPLINARY STUDIES, LAW AND MANAGEMENT

JADAVPUR UNIVERSITY
KOLKATA 700032
MAY 2019

JADAVPUR UNIVERSITY

FACULTY OF INTERDISCIPLINARY STUDIES, LAW AND MANAGEMENT

SCHOOL OF NUCLEAR STUDIES AND APPLICATION

CERTIFICATE OF RECOMMENDATION

This is to certify that the thesis entitled "**Study of Natural Convection Heat Transfer in an enclosure with a Heat Generating Porous Bed with Wall Temperature Variation**", which is being submitted by **Suman Modak** in partial fulfilment of the requirements for the award of the degree of "**Master of Nuclear Engineering"** at the School of Nuclear Studies and Application, Jadavpur University, Kolkata 700032, during the academic year 2017-2019, is the record of the student's own work carried out by him under our supervision.

Thesis Guide
Dr. Swarnendu Sen
Department of Mechanical Engineering
Jadavpur University, Kolkata 700032

Prof. (Dr.) Amitava Gupta
Director
School of Nuclear Studies and Application
Jadavpur University Kolkata 700032

Dr. Pankaj Kumar Roy
Dean
Faculty of Interdisciplinary Studies,
Law and Management
Jadavpur University Kolkata700032

JADAVPUR UNIVERSITY

FACULTY OF INTERDISCIPLINARY STUDIES, LAW AND MANAGEMENT

SCHOOL OF NUCLEAR STUDIES & APPLICATION

CERTIFICATE OF APPROVAL*

The foregoing thesis is hereby approved as a creditable study of an engineering subject carried out and presented in a manner satisfactory to warrant its acceptance as a prerequisite to the degree for which it has been submitted. It is understood that by this approval the undersigned do not necessarily endorse or approve any statement made opinion expressed or conclusion drawn therein but

approve the thesis only for the purpose for which it is submitted.

Committee on Final Examination
for Evaluation of the Thesis

Signature of Examiners

* Only in case the recommendation is concurred in

JADAVPUR UNIVERSITY

FACULTY OF INTERDISCIPLINARY STUDIES, LAW AND MANAGEMENT

SCHOOL OF NUCLEAR STUDIES & APPLICATION

DECLARATION OF ORIGINALITY& COMPLIANCE OF ACADEMIC ETHICS

*It is hereby declared that the thesis entitled "**Study Of Natural Convection Heat Transfer In An Enclosure With A Heat Generating Porous Bed With Wall Temperature Variation**" contains literature survey and original research work by the undersigned candidate, as part of his degree in Master of Nuclear Engineering.*

All information in this document has been obtained and presented in accordance with academic rules and ethical conduct.

It is also declared that all materials and results, not original to this work have been fully cited and referred throughout this thesis, according to rules of ethical conduct.

Name	:	SUMAN MODAK
Registration Number	:	141081 of 2017-18
Examination Roll Number	:	M4NUE19004

Dated:

(Signature)

ACKNOWLEDGEMENT

I want to gratefully acknowledge the resourceful guidance, active supervision and constant encouragement of Dr. Swarnendu Sen of Mechanical Engineering Department, Jadavpur University, who despite having other commitments could make time to help me to carry out this project. I do convey my true regards and gratitude to him. His excellent and patient assistance in the classroom lectures, have influenced me in the work.

I would like to take this opportunity to thank Prof. (Dr.) Amitava Gupta, Director, School of Nuclear Studies and Applications, Jadavpur University, without, whose initiative and support, it would not have been possible to carry out the project.

I owe many thanks and gratitude to Aranyak Chakravarty and Priyankan Datta, PhD students, Department of Mechanical Engineering, Jadavpur University who have provided very valuable technical guidance throughout the execution of the project, without their help in technical aspect and in different valuable discussion it may not be possible to come this far.

I also thankfully acknowledge the assistance received from all the research scholar of Project Neptune of Mechanical Engineering Department for their sincere, spontaneous and active support during the preparation of this work.

Millions of thanks go to my friends like Nillojendu Banerjee, Saheb Santra, Praneet Kumar Singh for the good moments we had shared during the time of working together, for their continuous support and for all our helpful discussions.

I would like to thank my parents. They have made very special impression in my personal life and that contributed to make this work possible. I am very grateful to my father, for his constant motivation, patience, encouragement, and for his love during these years. I also thank him for appreciating me for my work. I am also very grateful to my mother for her infinite mental support to me.

Dated: 28-05-2019 SUMAN MODAK

ABSTRACT

In case of a severe nuclear accident the biggest challenge for safety becomes the continuous removal of heat from the reactor core even after the termination of nuclear fission chain reaction. The radioactive fuel continues to produce decay heat even after the shutdown of the reactor. The heat continues to accumulate and a stage comes when extreme heat causes the core to melt down and form a heap like debris at the bottom of the reactor. At this stage if heat is still not removed it may lead to steam explosion and blasting off the containment building. So in this scenario the only possible way of heat removal is by natural convection which might prevent the situation from becoming catastrophic in nature.

The basic principle followed is once the molten fuel gathers at the bottom of the reactor to form a porous bed, water surrounding the heat generating porous bed absorbs heat and gets converted into vapour. The vapour which is lighter in density will rise up due to buoyancy and collide with the reactor walls. Once the vapour collides with the walls where it will deposit substantial amount of heat energy and then gets converted into liquid due to condensation and descend back to the bottom of the reactor. This process continues which ultimately sweeps out the decay heat which is generated continuously from the porous debris in the form of Natural Convection. The maximum amount of heat that can be removed from the bed is known as dryout of the debris bed and the corresponding power is known as dryout power.

Simulations were being conducted using the debris dryout model developed at Jadavpur University and using ANSYS FLUENT to find out the minimum dryout power and the effects of various sub cooling of wall temperatures at the given dryout power. An enclosure of size 0.3 m X 0.3 m with a heaped porous bed of a shape of a truncated cone of volume 0.0153 m^3 is taken. For each simulation a run time of 3600 seconds was performed. Simulations are also been conducted by varying the geometry of the debris bed keeping the volume of the bed constant. Variation of wall temperatures with varying debris geometry were also being performed to study the effect of dryout of the porous bed.

It was found that when the reactor walls were being maintained at various subcooled temperatures dryout condition of the porous debris bed was not observed although dryout condition was encountered when wall subcooling was not applied. So we can conclude that when we are able to maintain the wall at subcooled temperatures we can cool the reactor efficiently by the process of natural circulation.

Table of Contents

Table of Contents

List of Figures

LIST OF FIGURES

List of Tables

List of Abbreviations

RPV	:	Reactor Pressure Vessel
MFCI	:	Molten Fuel Coolant Interaction
MCCI	:	Molten Corium Concrete Interaction
CFD	:	Computational Fluid Dynamics
LTNE	:	Local Thermal non-equilibrium

Nomenclature

English alphabets

M	:	Mass Transfer Rate, $kg.s^{-1}$
C	:	Interfacial momentum exchange coefficient, $kg.m^{-3}.s^{-1}$
c_p	:	Specific heat capacity, J/kg.K
g	:	Acceleration due to gravity
h	:	Enthalpy, J/kg
q	:	Volumetric heat transfer rate, $W.m^{-3}$
S	:	Solid-fluid drag force, $kg.m^{-2}.s^{-2}$
T	:	Temperature, K
V	:	Velocity , $m.s^{-1}$
p	:	Pressure, Pa

Greek Symbols

α	:	Volume fraction
β	:	Thermal conductivity, $W.m^{-1}.K^{-1}$
ε_f	:	Porosity
μ	:	Dynamic Viscosity (kg/m.s)
ρ	:	Density (kg/m^3)

Subscripts / Superscripts

v	:	Vapour phase
i	:	interface
l	:	Liquid phase
s	:	Solid phase
< >	:	Eulerian volume-averaged quantities
sat	:	saturated

Chapter 1

INTRODUCTION

1.1 OVERVIEW OF THE TOPIC

With advancement of age the need of renewable energy in the form of nuclear energy is becoming more and more. With increase in population the demand for clean energy is rising rapidly as a result there is an increase in the number of nuclear power plants. With the increase in the number of nuclear power plants we have to be very careful regarding the safety of the nuclear power plants. In case of any unfortunate events we have to prepare ourselves in case of a severe nuclear accident.

The biggest problem of a running nuclear reactor is that it continues to generate decay heat even after ending the nuclear fission chain reaction. After the shutdown of the nuclear reactor it still produces 6% of the thermal power and even after one hour it continues to produce 1% of the thermal power. So the challenge lies in continuous removal of decay heat which is being generated still after the shutdown of the reactor. If the decay heat is not removed continuously there will be an accumulation of heat energy which will result in sharp increase in the temperature of the reactor core and will lead to its meltdown.

Generally in case of a severe nuclear accident there is a stoppage of normal along with emergency core cooling system which leads to accumulation of heat energy. As a result there is an enormous amount of rise in temperature which leads to evaporation of water inside the reactor core. This loss of water exposes the fuel rods to the air which further decreases the heat transfer from the fuel elements. In such a scenario the tremendous amount of accumulated heat can cause meltdown of the fuel rods along with its structure.

When the core meltdown takes place which is commonly known as the corium will descend down towards the bottom of the reactor pressure vessel (RPV) due to the action of the gravity. The molten core falls in the form of jets and accumulates at the bottom of the reactor to form a molten mass. When the molten core falls through the residual water inside the core it experiences a hydrodynamic force which leads to fragmentation of the molten particles which is known as hydrodynamic fragmentation. At this point of time the temperature rises so much that film boiling of the residual water initiates which causes the water vapour to cover up the fragmented molten particles. When the vapour envelope breaks down

the hot molten particles are exposed to the surrounding water. This leads to a generation of thermal stress in the particles and causes local pressurization which leads to secondary fragmentation of the molten particles which is known as thermal fragmentation. The fragmented particles eventually settle down at the bottom of the RPV and quenches down. This is known as Molten Fuel Coolant Interaction (MFCI). Since this action is taking place inside the RPV it is known as In-Vessel phase of the accident progression sequence.

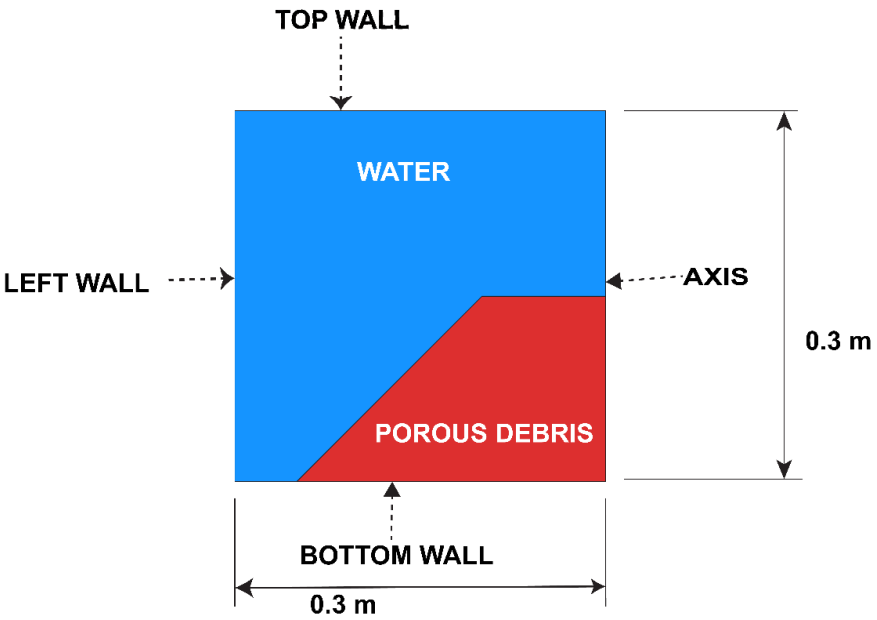

Figure 1.1 Schematic diagram of the problem geometry

When the molten fuel breaches the wall of the RPV and enters into the containment it is termed as Ex-Vessel Phase as the incident is taking place outside the RPV. At this point of time cooling of the ex-vessel debris formed at the base of the containment is very vital. Failure to do so will initiate molten corium concrete interaction (MCCI) which will lead to the release of radioactivity in the environment. A schematic diagram drawn below represents the sequence of events during a severe nuclear accident.

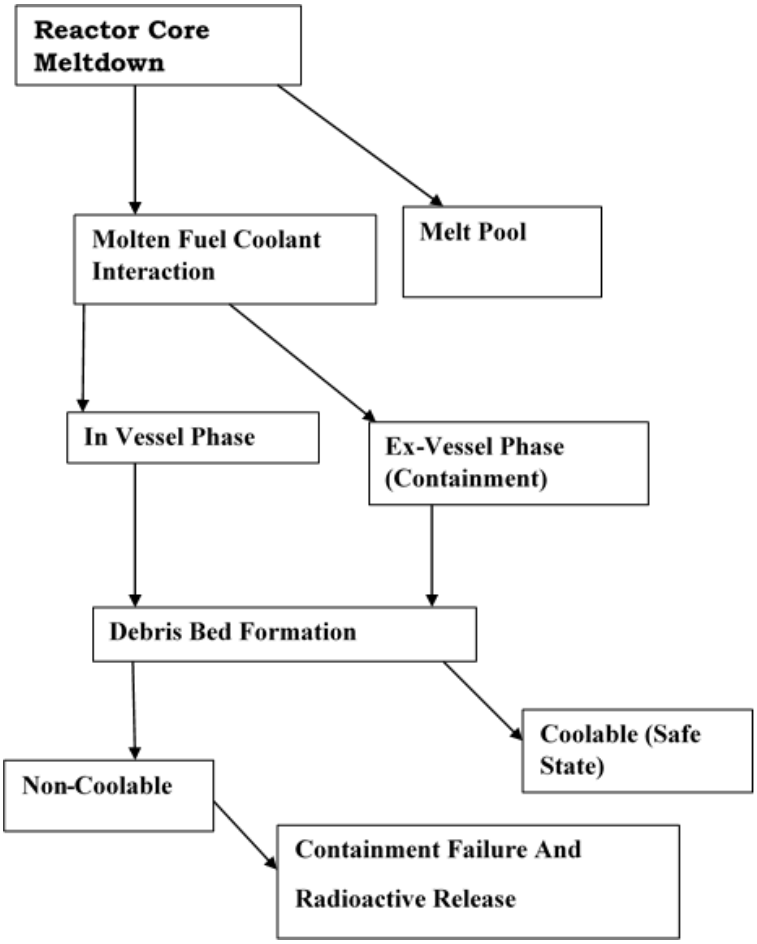

Figure 1.2 Schematic representation of accidental progression sequence considering molten fuel coolant interaction.

1.2 LITERATURE REVIEW

1.21 COOLING OF THE CORE

Depending on the type of reactor and the corium composition a power density of 0.5 MW/m^3 to 1.5 MW/m^3 is generated which can only be removed by boiling heat transfer using cold water. In order to maintain a stable coolable condition of the molten core either relentless supply of cold water has to be introduced from outside or else evaporation and condensation of re-circulated water has to be done continuously to remove the heat energy.

The first process of core cooling is pretty useful when there is no problem with working of primary and emergency core cooling system. But when there is non-availability of electricity which would prevent the driving of the respective pumps the second process of core cooling by evaporation and condensation becomes handy. The process involves when cold water either injected from outside or some residual water present inside the core will absorb the heat energy from the hot molten fuel

and evaporate into vapour. When the vapour which is ascending strikes the cold wall surfaces and deposit the heat energy over there. After losing the heat, the vapour converts into water by condensation and descends into the reactor core again. This process continues without the aid of electric power and cools the reactor core substantially.

1.22 DRYOUT POWER AND DRYOUT HEAT FLUX

In case if there is a failure to maintain the core in a coolable condition then due to the heat generating nature of the corium, high amount of heat is generated inside the fuel which will increase the temperature of the debris bed. This might lead to re-melting of the debris and form a molten pool again. The molten pool will interact with the bottom wall of RPV and in certain cases might lead to a breach in the RPV walls and flow into the containment. When the molten pool flows into the containment it again undergoes hydrodynamic fragmentation and thermal fragmentation on coming in contact with water. If the accident progression is not terminated at this stage it will lead into steam explosion and complete failure of the containment. This effect will be catastrophic in nature as the radioactivity will be released into the outside world. So it becomes very necessary to provide proper cooling of the debris bed in order to arrest the accident progression.

So it becomes very important to have an assessment beyond which the debris cannot be maintained at a coolable condition. This limit is known as the dryout condition. The heating power associated with it is known as dryout power and the maximum heat flux that can be removed from the debris bed is known as dryout heat flux.

1.23 CHARACTERISTICS OF DEBRIS BED

The occurrence of dryout in debris bed is significantly influenced by system pressure, coolant temperature, coolant flooding mechanism as well as composition, structure of debris beds (Magallon And Huhtiniemi 2001; Magallon 2006).Debris bed characteristics is related to the composition and structure of the debris bed which is formed in the event of a severe nuclear accident. It is a very important aspect as far as coolability of debris bed is concerned. Several experiments conducted in the past have revealed that due to molten fuel coolant interaction fragmented mass of debris is formed which has a irregular and non-homogeneous porous composition. It is reported that the porosity of debris bed is found to be between 0.25 and 0.7 and the size of the fragments is found to be between hundred microns to approximately 50 mm. The porosity of the bed allows coolant movement through the interconnected voids which helps it to extract heat energy from the debris bed and allows to cool down.

It is also observed in experiments that generally when molten jet particles are fragmented due to hydrodynamic fragmentation and thermal fragmentation it tends to form a heap shaped debris bed. The tendency to form a heap shaped debris bed also increased with increase in particle size as seen from experiments by Lin et al.(2017). There were some uncertainty about the structure of the formation of the debris bed but it was expected to form a heap like structure Karbojian et al. (2009). Recently experiments were conducted and it was found that for fine particle size of less than 0.25 mm flat topped cylindrical bed was formed Lin et al. (2017). When the particle size was increased to 2.5 mm and beyond the bed shape became convex shaped conical bed Lin et al. (2017).

It is also found from experimental investigation that the dryout is influenced immensely by the size and composition of the porous debris bed Squarer et al. (1982). Dryout heat flux becomes larger with increased particle sizes. Porosity also impacts the dryout heat flux significantly as reported by Ma and Dinh (2010).

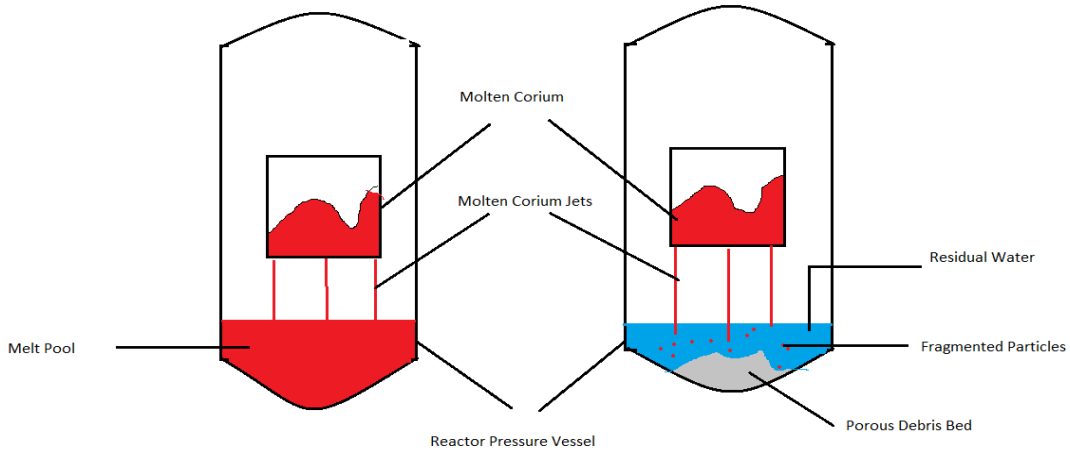

Figure 1.3 (left) Schematic representation of molten corium flooding the lower part of the reactor. (right) Formation of porous debris bed at the bottom of the reactor

1.24 DRYOUT OCCURRENCE AND IT'S CONTRIBUTING FACTORS

Estimation of the dryout power is a vital point as per coolability of the debris bed is concerned. One of the significant causes of dryout is that when the residual water or cold water injected from outside interacts with the hot debris bed it evaporates to form water vapour due to high amount of heat transfer between them. The water vapour formed is lighter in weight and due to buoyancy it starts to rise up through the debris. On the other hand fresh set of cold water injected from outside tries to descend down inside the debris bed. When a large amount of water vapour is formed it stops the ingression of cold water into the debris bed. The hot vapour locks

out the cold water from reaching the bottom of the debris bed and prevent it from cooling down. This counter current movement of cold water and hot vapour causes the dryout of the debris bed. Generally the dryout occurance is exhibited at the top of the debris bed.

It is seen from experiments conducted previously that Dryout Heat Flux (DHF) increases with the increase in pressure. The work regarding the influence of pressure on DHF was reported by Squarer et al. (1982) , Reed et al. (1986) , Miyazaki et al. (1986) , (Lindholm et al. 2006) and (Schafer et al. 2006a , 2006b)

The composition of the porous bed also have an impact on the dryout occurance. Reports obtained from (Schafer et al 2006a , 2006b) suggest that DHF increases with increase in particle size. Porosity of debris bed also have a strong impact on DHF.

1.25 VARIOUS TYPES OF DEBRIS BED COOLING

Dryout Heat Flux (DHF) is very much depended upon the modes of fluid flow inside the debris bed. One of the chief contributing factor towards dryout phenomenon is counter current fluid flow due to top flooding mechanism of the reactor core. If co-current fluid flow is realised by introducing bottom flooding or lateral flooding DHF increases substantially due to better cooling effect.

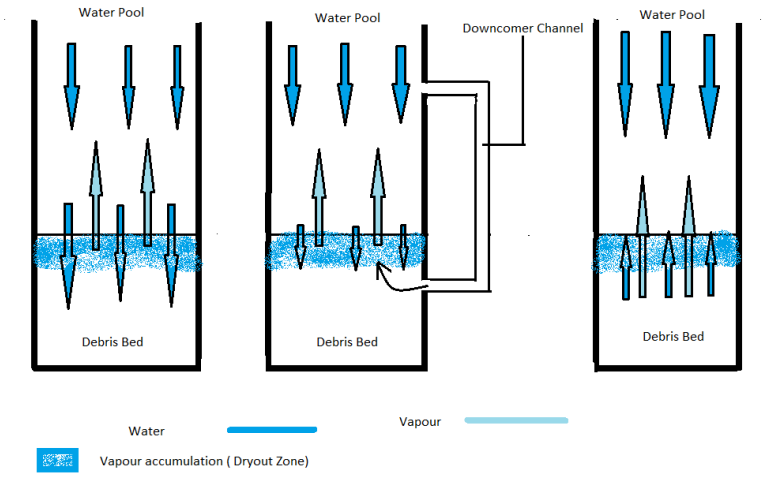

Figure 1.4 Schematic representation of (left) Top flooding and counter-current flow of water and vapour. (center) Lateral flooding and (right) Bottom flooding in one dimensional debris beds

In the bottom flooding mechanism cold water is injected from the bottom of the debris bed and in lateral flooding mechanism cold water is injected from the lateral surface of the bed. In these two mechanisms the ascending vapour from the debris is not blocked from moving up by the rushing cold water. As a result the hot vapour is allowed to escape from the high temperature bed taking out ample amount of heat with it, simultaneously fresh set of coolant is able to reach to the bottom of

the bed to provide sufficient coolability. Thus the dryout limit of the bed is increased substantially.

In Fig. 1.4 (left) top flooding of the debris by water is shown. The counter-current movement of water and water vapour is leading to vapour accumulation at the top of the surface. In order to increase the dryout limit the co-current movement of water and water vapour is to be employed. This can be achieved as shown in figure (center) and (right).

In figure (center) lateral flooding is employed as the evaporated water is cooled and condensed and again sent back to the bottom of the reactor vessel via the downcomer channel from the lateral surface of the debris bed.

In figure (right) bottom flooding is employed as fresh coolant is injected from the bottom of the debris bed to facilitate more heat transfer.

The above two methods of lateral flooding and bottom flooding induces co-current movement of steam and water and thus increases the heat transfer rate from the bed and thus augments the dryout limit of the debris bed.

When coolant is injected from both bottom,lateral and top surfaces of the bed it is known as multi-dimensional cooling. It is reported from several experiments that multi-dimensional cooling of the bed is very much effective as compared to one-dimensional cooling. Studies have shown that DHF increases several times when multi-dimensional cooling is implemented as compared to one-dimensional cooling.Multi-dimensional flooding effects on coolability of debris bed was carried out in 1988 by Wang and Dhir. It was observed that coolant injection from the bottom of the debris bed along with top flooding was more effective than top flooding alone. Later in 2010 Ma and Dinh reported an increase in dryout heat flux around 40% with bottom flooding situations as compared to the top flooding. Multi-dimensional flooding increased the dryout limit several times as compared to top flooding of the bed surface. Multi-dimensional flooding is shown below.

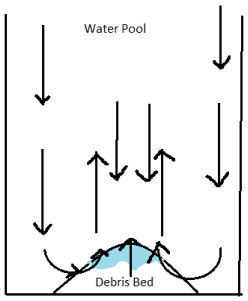

Figure 1.5 Multidimensional flooding associated with heap like debris bed

Reports from (SARNET) indicated that when a debris bed of non-homogeneous structure and shape is being formed coolability is improved when coolant flow from sides and bottom are being introduced that is two dimension/three dimension effects are being applied rather than one dimensional situation with top flooding. From studies conducted by Burger et al. The debris bed formed due to a severe nuclear accident by break-up of melt jets in water is multi-dimensional in nature. They investigated situations with downcomers and ex-vessel situation.

In respect to heat removal from the debris by natural convection, a debris bed was assumed to be located centrally at the bottom of a cylindrical steel container Chakravarty et al. (2017). The shape of the debris bed was modeled as a truncated cone such that symmetry was assumed along z-axis. The bottom wall was assumed adiabatic in nature and the top and side walls of the enclosure was kept at constant temperature. It is assumed that walls are impermeable in nature. It is assumed that the debris particles are spherical in nature and generating heat. Also the debris bed are surrounded by water at saturation temperature initially. The porosity of the debris particles was 0.39 and diameter of the particles was around 0.95 mm. The study was conducted for a corresponding power density of 1305.45 KW/m^3 and a system pressure of 1.3 bar Chakravarty et al. (2017).

Due to heat generation from the debris bed a buoyancy motion is induced as a result water and the heated vapour is moving in a counter-clockwise motion. These fluid motions are causing heat transfer from the hot debris to the cold enclosure walls. The heat transfer is taking place by convective fluid motion and by conduction across the porous fluid interfaces. With heat transfer taking place continuously water vapour is generated and it rises to the top of the enclosure and transfers the heat energy. The vapour is then deflected to the side walls of the enclosure and transfers a substantial amount of heat energy. The vapour then gets cooled comes to the lower portion of the enclosure to repeat the process again. Thus a counter-clockwise motion is being set inside the enclosure by steam and water. In case the fluid motion is unable to remove the required amount of heat from the corium dryout will occur. In case of a dryout the corium will be devoid of any water and heat transfer rate reduces significantly. This will further lead to rapid rise of temperature of the debris bed Chakravarty et al. (2017).

It is seen that if the enclosure walls are maintained at sub-cooled temperatures (that is well below the saturation temperature) a certain temperature difference is created between bulk fluid and the wall. This leads to transfer of heat energy from the debris continuously and coolability can be ensured Chakravarty et al. (2017).

As per experiments conducted by Lee and Suh (2003) with high Rayleigh Number turbulent natural convection in the Mini-SIGMA tests in a two dimension semi-circular slice pool. It was observed that when insulation was provided to the top surface of the pool heat flux increases to about 6%. When the upper boundary was

maintained at adiabatic condition the heat was transferred from the pool by buoyancy induced flow was to the side-wards instead of upper boundary at the top.

MFCI helps to disintegrate the molten corium into small particles which lead to increase in the surface area of the porous bed formed. This increases the cooling surface of the porous bed which leads to better coolability. One of the striking features of an experiment conducted in DAVINCI test facility where air bubbles were injected from the bottom of the test bed which stimulates steam flow. It was observed that once the air bubbles collide with finely disintegrated molten particles poured from the top (which is representing the molten corium descending down in case of a severe accident), the molten particles spreads out. As a result it forms a porous bed with high lateral growth and limited vertical growth at the centre. When no air bubbles were injected from the bottom it resulted in formation of a bed which has a higher vertical growth and lower lateral growth. So the study by Kim et al.(2016) showed two phase natural convection affects the formation of the debris bed. Similarly studies from Yakush et al.(2008, 2009) showed two phase natural convection causes spreading out of the particles and a porous structure is formed which increases the surface area to the coolant and delays the dryout of the bed.

From experimental investigation as reported by Takasuo et al.(2016) that debris formed which has a heap like structure with a greater height than a flat shaped debris will cause presence of local steam fluxes at the apex which will make the top portion vulnerable to dryout. In the case of a bed with relatively lower height and same volumetric power generation the maximum steam flux at the top is always smaller which will render the area less prone to dryout. From COOLOCE experiment it was observed that mass flux of steam which is responsible for dryout increases with bed height

An interesting observation was made on coolability of the debris bed with variation in the geometry. A conical shaped bed and a cylindrical shaped with same porosity , volume and radius was considered with multi-dimensional flooding of the coolant. The height of the cylinder was taken three times that of the cylinder. It was reported that at all pressures the dryout power density for the cylinder shaped bed was greater by 89%-100% as compared to conical bed. It was seen that power density for cylinder must increase in order to reach the dryout heat flux.

Kulkarni et al.(2010) have performed experiments and found that pressure and coolant flow rate influences DHF. It was reported that with low coolant flow rates and bottom flooding conditions coolability of debris bed is limited by counter-current flooding limit.

1.3 OBJECTIVE

As per the discussions of the previous sections we can easily state that after an occurrence of a severe nuclear accident the coolability of the porous debris bed formed is of utmost importance. This is because of the fact that adequate cooling of the debris

will terminate the accident progression sequence and will help to stabilise the situation. As soon as the accident progression is terminated the danger of releasing the radioactive product to the outside world will come to a halt.

Coolability of a debris bed which is capable of an energy production of around few hundred megawatts is no easy task especially when there is no power to operate the core cooling system. At this situation cooling the core by natural convection is the only mode available. The objective of the current work is to study the effect of natural convection on debris coolability. For this purpose, the commercial CFD tool ANSYS FLUENT 14.5 is used. Efforts have been made to study the effects of variation of wall temperature on the coolability of the bed. In the present work, an attempt has been made to find out the dryout heat flux when the wall temperature was varied. Study has also been conducted on the effect of pressure variation on the dryout heat flux.

Chapter 2

DEVELOPMENT OF MODEL TO ANALYSE MULTIPHASE FLOW IN THE HEAT GENERATING POROUS SYSTEM

2.1 OVERVIEW OF DEBRIS MODEL

The debris dryout model has been developed at the Jadavpur University to study the phenomenon of natural convection heat transfer in an enclosure with a heat generating debris bed. To study the effect of multiphase flow and dryout phenomenon in debris bed we need to solve the mass equation, momentum equation and energy equation in the clear fluid region meant for liquid and the vapour phases and also the porous debris bed region.

The porous nature of the debris bed facilitates the movement of the fluid through it as a result the fluid experiences some drag force. So the drag laws can be applied for modelling of the momentum transfer in the porous bed. For modelling the energy transport between the heat generating debris bed and the fluid region local thermal non-equilibrium model (LTNE) has been adapted. The assumptions made while developing the model are given below:

1. Heat generation takes place in the solid debris particles only.
2. The effects of capillary pressure are not considered in the development of model, that means all the constituent of fluid phases have the same static pressure $p_l = p_v = p$.
3. The porous medium forming the debris bed is homogeneous and isotropic in nature.
4. The thermo-physical properties of all the phases are constant except the density of the fluid phases which are modeled using the Boussinesq approximation.

2.2 GOVERNING EQUATIONS FOR THE CLEAR FLUID REGION

Mass transport:

$$\frac{\partial}{\partial t}(\alpha_v \rho_v) + \nabla.(\alpha_v \rho_v \langle \boldsymbol{V}_v \rangle) = M_{lv}''' \tag{2.1}$$

$$\frac{\partial}{\partial t}(\alpha_l \rho_l) + \nabla.(\alpha_l \rho_l \langle \boldsymbol{V}_l \rangle) = M_{vl}''' \tag{2.2}$$

such that $M_{lv}''' = -M_{vl}'''$.

Momentum transport:

$$\frac{\partial}{\partial t}(\alpha_v \rho_v \langle \boldsymbol{V}_v \rangle) + \nabla.(\alpha_v \rho_v \langle \boldsymbol{V}_v \rangle \langle \boldsymbol{V}_v \rangle) = -\nabla(\alpha_v p) + \mu_v \nabla^2 \langle \boldsymbol{V}_v \rangle + M_{lv}''' \langle \boldsymbol{V}_{lv} \rangle + C_{lv}(\langle \boldsymbol{V}_l \rangle - \langle \boldsymbol{V}_v \rangle) + \alpha_v \rho_v \boldsymbol{g} - \nabla.(\rho_v \langle \boldsymbol{V}_v' \boldsymbol{V}_v' \rangle) \tag{2.3}$$

$$\frac{\partial}{\partial t}(\alpha_l \rho_l \langle \boldsymbol{V}_l \rangle) + \nabla.(\alpha_l \rho_l \langle \boldsymbol{V}_l \rangle \langle \boldsymbol{V}_l \rangle) = -\nabla(\alpha_l p) + \mu_l \nabla^2 \langle \boldsymbol{V}_l \rangle + M_{vl}''' \langle \boldsymbol{V}_{vl} \rangle + C_{vl}(\langle \boldsymbol{V}_v \rangle - \langle \boldsymbol{V}_l \rangle) + \alpha_l \rho_l \boldsymbol{g} - \nabla.(\rho_v \langle \boldsymbol{V}_l' \boldsymbol{V}_l' \rangle) \tag{2.4}$$

Energy transport:

$$\frac{\partial}{\partial t}(\alpha_v \rho_v \langle h_v \rangle^v) + \nabla.(\alpha_v \rho_v \langle \boldsymbol{V}_v \rangle \langle h_v \rangle^v) = \alpha_v \beta_v \nabla^2 \langle T_v \rangle - \langle q_{vi}''' \rangle + M_{lv}''' \langle h_{vi} \rangle^v - \nabla.(\rho_v \langle h_v' \boldsymbol{V}_v' \rangle) \tag{2.5}$$

$$\frac{\partial}{\partial t}(\alpha_l \rho_l \langle h_l \rangle^l) + \nabla.(\alpha_l \rho_l \langle \boldsymbol{V}_l \rangle \langle h_l \rangle^l) = \alpha_l \beta_l \nabla^2 \langle T_l \rangle - \langle q_{li}''' \rangle + M_{vl}''' \langle h_{li} \rangle^l - \nabla.(\rho_l \langle h_l' \boldsymbol{V}_l' \rangle) \tag{2.6}$$

2.3 GOVERNING EQUATIONS FOR THE DEBRIS BED REGION

Mass transport:

$$\frac{\partial}{\partial t}\left(\varepsilon_f \alpha_v \rho_v\right) + \nabla.(\alpha_v \rho_v \langle \boldsymbol{V}_v \rangle) = M_{lv}''' \tag{2.7}$$

$$\frac{\partial}{\partial t}\left(\varepsilon_f \alpha_l \rho_l\right) + \nabla.(\alpha_l \rho_l \langle \boldsymbol{V}_l \rangle) = M_{vl}''' \tag{2.8}$$

such that $M_{lv}''' = -M_{vl}'''$.

Momentum transport:

$$\frac{\partial}{\partial t}(\alpha_v \rho_v \langle \boldsymbol{V}_v \rangle) + \nabla.\left(\frac{\alpha_v \rho_v \langle \boldsymbol{V}_v \rangle \langle \boldsymbol{V}_v \rangle}{\varepsilon_f}\right) = -\nabla\left(\varepsilon_f \alpha_v p\right) + \mu_v \nabla^2 \langle \boldsymbol{V}_v \rangle + \frac{1}{\varepsilon_f}\left(M_{lv}''' \langle \boldsymbol{V}_{lv} \rangle + R_{lv}(\langle \boldsymbol{V}_l \rangle - \langle \boldsymbol{V}_v \rangle)\right) + \varepsilon_f \alpha_v \rho_v \boldsymbol{g} + \langle \boldsymbol{S}_{sv} \rangle \quad (2.9)$$

$$\frac{\partial}{\partial t}(\alpha_l \rho_l \langle \boldsymbol{V}_l \rangle) + \nabla.\left(\frac{\alpha_l \rho_l \langle \boldsymbol{V}_l \rangle \langle \boldsymbol{V}_l \rangle}{\varepsilon_f}\right) = -\nabla\left(\varepsilon_f \alpha_l p\right) + \mu_l \nabla^2 \langle \boldsymbol{V}_l \rangle + \frac{1}{\varepsilon_f}\left(M_{vl}''' \langle \boldsymbol{V}_{vl} \rangle + C_{vl}(\langle \boldsymbol{V}_v \rangle - \langle \boldsymbol{V}_l \rangle)\right) + \varepsilon_f \alpha_l \rho_l \boldsymbol{g} + \langle \boldsymbol{S}_{sl} \rangle \quad (2.10)$$

Energy transport:

$$\frac{\partial}{\partial t}\left(\varepsilon_f \alpha_v \rho_v \langle h_v \rangle^v\right) + \nabla.\left(\alpha_v \rho_v \langle \boldsymbol{V}_v \rangle \langle h_v \rangle^v\right) = \alpha_v \varepsilon_f \beta_v \nabla^2 \langle T_v \rangle + \langle {q_{sv}}''' \rangle - \langle {q_{vi}}''' \rangle + {M_{lv}}''' \langle h_{vi} \rangle^v \quad (2.11)$$

$$\frac{\partial}{\partial t}\left(\varepsilon_f \alpha_l \rho_l \langle h_l \rangle^l\right) + \nabla.\left(\alpha_l \rho_l \langle \boldsymbol{V}_l \rangle \langle h_l \rangle^l\right) = \alpha_l \varepsilon_f \beta_l \nabla^2 \langle T_l \rangle + \langle {q_{sl}}''' \rangle - \langle {q_{li}}''' \rangle + {M_{vl}}''' \langle h_{li} \rangle^l \quad (2.12)$$

Energy transport for solid particles:

$$\frac{\partial}{\partial t}\left(\left(1 - \varepsilon_f\right)\rho_s c_{p,s} \langle T_s \rangle\right) = (1 - \varepsilon_f)\beta_s \nabla^2 \langle T_s \rangle + \langle {q_s}''' \rangle - \langle {q_{sl}}''' \rangle - \langle {q_{sv}}''' \rangle - \langle {q_{si}}''' \rangle \quad (2.13)$$

2.4 MASS TRANSFER ASSESSMENT

Interfacial mass transfer between the liquid and vapour phases is evaluated using the boiling heat flux and interfacial heat fluxes as shown below

$${M_{lv}}''' = \frac{\langle {q_{s,i}}''' \rangle + \langle {q_{v,i}}''' \rangle + \langle {q_{l,i}}''' \rangle}{h_{v,sat} - h_{l,sat}} \quad (2.14)$$

For the remaining equations and text regarding the modelling can be referred from Chakravarty (2018).

2.5 CLOSURE RELATION

Appropriate closure relations are required for proper modeling of the interfacial drag terms in the momentum transport equations as well as the heat transfer terms in the energy transport equations. The closure relations adopted in the present analysis are listed below in the table.

Table 2.1 Closure Term and Correlation

Momentum Transfer	Interfacial drag in clear fluid region	Schiller and Naumann
	Interfacial drag in clear fluid region	Schulenberg and Muller
Heat Transfer	Convection to Liquid	Ranz and Marshall
	Boiling	Rhosenow (Nucleate Boiling) Bromley (Film Boiling)
	Convection to Vapour	Ranz and Marshall
	Interfacial Liquid-Vapour Heat Transfer	Ranz and Marshall

2.6 NUMERICAL PROCEDURE

The volume averaged governing equations are implemented within the framework of ANSYS FLUENT with the use of Eulerian multiphase model and the porous media model. The solid energy transport equation is solved separately as a user-defined transport equation. The closure relations detailed in Section 4.4 are also implemented in ANSYS FLUENT with the help of user-defined functions. The numerical schemes used in solving the governing equations are listed in the table below. The solution obtained is estimated to be converged if the magnitude of all residuals are below 10^{-4}.

Table 2.2 UDF modules utilised in implementation of the model

Quantities	UDF Module
Interfacial momentum exchange coefficient	DEFINE_EXCHANGE_PROPERTY
Relative permeability and relative passability	DEFINE_PROFILE
Heat transfer terms	DEFINE_SOURCE
Mass transfer	DEFINE_MASS_TRANSFER
Transient term in Eq. 5.13	DEFINE_UDS_UNSTEADY
Diffusive term in Eq. 5.13	DEFINE_DIFFUSIVITY

Chapter 3

RESULTS AND DISCUSSIONS

3.1 PROBLEM DESCRIPTION

In the present study simulations are being conducted using the debris dryout model developed at Jadavpur University and are executed using the ANSYS FLUENT 14.5. An enclosure of size 0.3m x 0.3m is with a heaped porous bed of a shape of a truncated cone of volume 0.0153 m^3 is taken. For every simulations a run time of 3600 seconds were performed to give a substantial amount of time so that the system will get stabilized. In the present study an unstructured computational grid of 3 mm nominal cell size (9560 cells in the entire domain) and a time-step size of 10^{-3}s is used for computations. A criterion of all residuals below 10^{-4} is followed for determining convergence of the numerical solution. The numerical schemes followed for solving the implemented governing equations are listed in Table 3.1 below.

Table 3.1 Numerical schemes adopted for simulation

Parameter	Scheme
Pressure-Velocity Coupling	Phase-Coupled SIMPLE
Gradient	Least Squares Cell Based
Momentum, Turbulent Kinetic Energy, Turbulent Dissipation Rate, Energy, UDS	Second Order Upwind
Volume Fraction	QUICK
Transient Formulation	Bounded Second Order Implicit

The walls of the enclosure are formed of steel with the given conditions that the top and left wall are kept at constant temperature and the bottom wall is adiabatic in nature.

The fluid used is water and appropriate properties are used depending upon the required conditions. The material properties used for the debris particles are given below.

Table 3.2 Material properties assumed for the solid particles (Takasuo et al. 2014)

Property	Magnitude
$\boldsymbol{\rho_s}$	4200 $kg.m^{-3}$
$\boldsymbol{\beta_s}$	2 $W.m^{-1}.K^{-1}$
$\boldsymbol{c_{ps}}$	775 $J.kg^{-1}.K^{-1}$

3.2 Assessment of Bed Coolability

While assessing the coolability of the heat generating porous bed it is very important to identify the occurrence of dryout inside the bed as it would it give us a measure of maximum limit of bed cooling at a particular condition.

The detection of the dryout in the present study can be identified by the change in two parameters that is minimum liquid saturation ($\alpha_{l,min}$) and maximum solid temperature ($T_{s,max}$) inside the debris bed. The dryout condition of the bed is achieved if the following two conditions are satisfied :

(1) The minimum liquid saturation inside the bed should become zero. Once it becomes zero the value should remain constant for the rest of the time.
(2) The maximum solid temperature should increase at least 5K above the steady state condition.

The volumetric heat generation rate at which dryout is observed is identified by initially carrying out simulations at low heat generation rates and then gradually increasing it until dryout is obtained. This is referred to as the dryout power density and the corresponding total heat generation rate as the dryout power.

3.3 STUDY OF MULTIPHASE FLUID FLOW AND HEAT TRANSFER LEADING TO DRYOUT

In the present study of multiphase fluid flow and heat transfer leading to dryout in truncated debris bed the following points are discussed as following.

The volume of the truncated bed is 0.0153 m^3 while the diameter of the particles of the bed is 0.001 m. The top radius and bottom radius of the bed are 0.1 m and 0.25 m respectively. The height of the bed is 0.15 m while the angle of the bed 45 degree. In addition, the permeability of the bed is 1.185 X 10^{-9} m^2 and the passability is 6.095 X 10^{-5} m.

The simulations are conducted for pressure of 1 bar and 2 bar only. For 1 bar pressure the enclosure is filled with liquid saturated water at saturation temperature of 372.7559 K. The solid debris is also assumed to be at saturation temperature initially. Similarly for 2 bar pressure, the liquid and solid particles initially exists at saturation temperature of 393.36 K. It is to be noted that phase 1 is considered as water and phase 2 is considered as water vapour. The top wall and the left wall are made of steel and are maintained at constant saturation temperature while the bottom wall is adiabatic in nature.

When the simulation is conducted for subcooled condition that is temperature decreased from the given saturation temperature at a given pressure, the wall temperature and the water temperature is maintained at the given subcooled temperature.

Due to heat generation nature of the debris, the temperature of the solid particles start to increase rapidly and it results in convective heat

transfer from the solid to liquid phase. The liquid phase on receiving heat energy starts heating up and temperature ascends quickly. As soon as liquid reaches saturation temperature boiling initiates and vapour generation commences. At this point of time heat transfer from solid to vapour and liquid to vapour due to convection results in a very high rate of transfer of heat energy. This continues and eventually a temperature gradient is being set-up in the enclosure. Vapour formed inside the debris picks up the heat and ascends up to the top due to buoyancy driven motion of the fluid phases.

3.4 RESULTS

Case 1 *When simulation was conducted at 1 bar pressure for 3600 seconds*

For the given 1 bar pressure the initial temperature of top wall, left wall, water and the debris are maintained at saturation temperature of 372.7559 K. After a series of trial it was found that the minimum dryout power for 1 bar pressure for a run time of 3600 seconds is 15 kW. At the time duration of 3340 seconds dryout phenomenon was observed. Dryout was marked with vapour accumulation at the top of the bed and a steep rise in solid temperature.

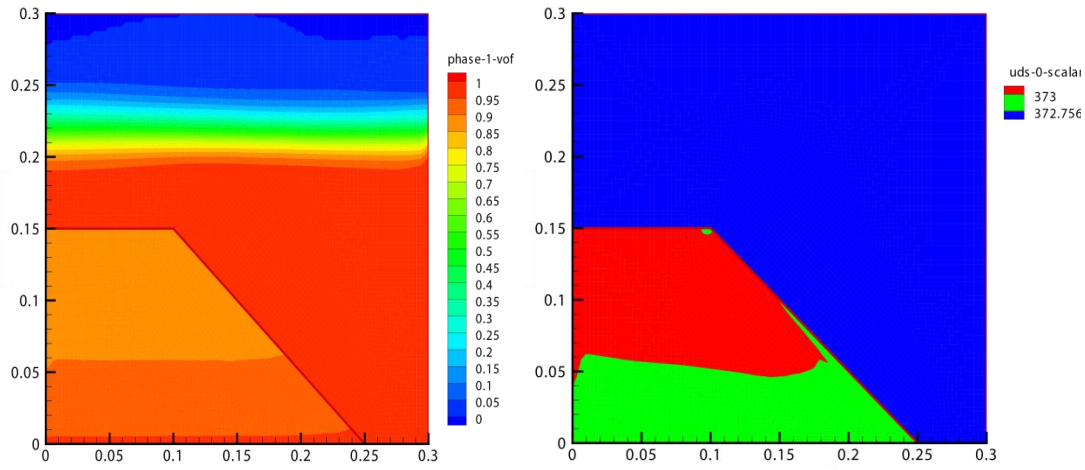

(a) **(b)**

Figure 3.1 (a) No vapour accumulation in the debris bed at 2000 sec; (b) Bed temperature at 2000 sec.

Heat generation inside the solid results in increase in temperature of the debris bed. The heat is transferred to the surrounding liquid due to convection as a result temperature of the liquid starts to rise. Once the liquid temperature reaches the saturation temperature it starts to boil and results in formation of vapour. Heat

transfer starts to take place between solid to vapour and from vapour to liquid. In the above figure 3.1 we can see that although vapour is starting to form inside the bed the temperature of the bed lies very close to saturation temperature. Thus it implies that as the heat from the bed is removed sufficiently the temperature of the bed is not rising.

It is clearly seen from the above figure 3.1 that dryout was not achieved at 2000 seconds because there is no vapour accumulating inside the bed.

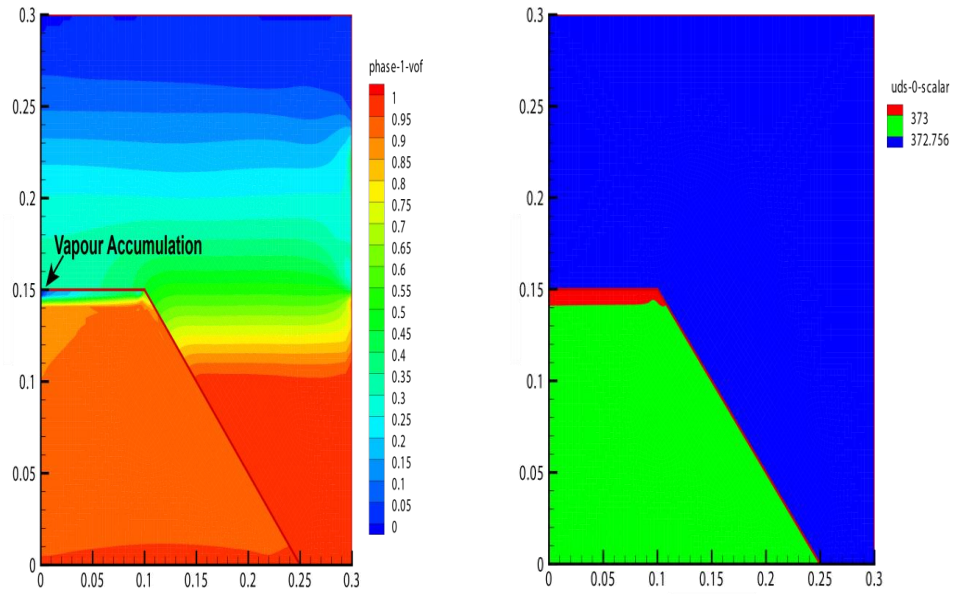

(a) **(b)**

Figure 3.2 (a) Development of dryout in the debris bed at 3340 sec in terms of liquid saturation and(b) bed temperature at 3340 sec.

This heat removal process continues until a stage comes when it reaches a limit beyond which the debris cannot be maintained in a coolable state. This is known as dryout condition. In the figure 3.2 we can see that dryout point has been attained and since heat is accumulating inside the bed the temperature of the bed is rising.

From the figure 3.3 we can clearly see that after certain amount of time has elapsed after attaining dryout, vapour is accumulating at the top of the bed. The temperature of the bed has also risen significantly as adequate cooling cannot be done.

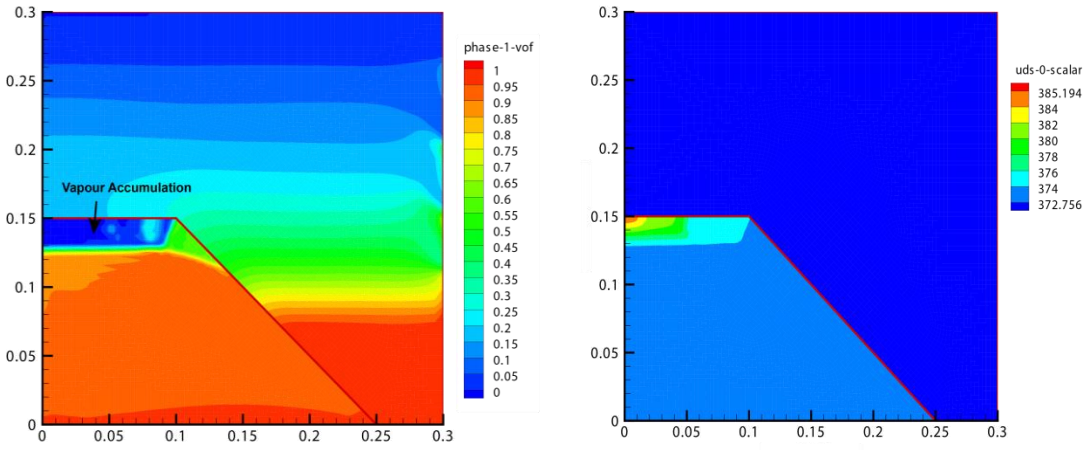

(a) **(b)**

Figure 3.3 (a) Volume of fluid in the debris bed at 3600 sec; (b) Solid Temperature of the bed at 3600 sec

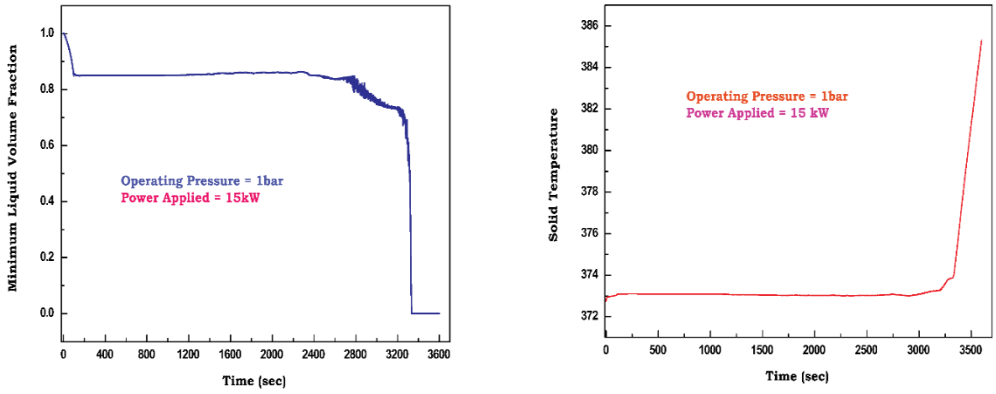

(a) **(b)**

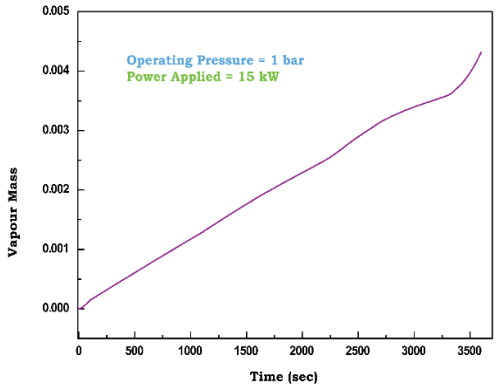

(c)

Figure 3.4 (a) shows minimum liquid volume fraction versus time inside the debris bed; (b) shows maximum solid temperature versus time inside the debris bed; (c) shows vapour mass generated versus time inside the debris bed

It is clearly seen from the above figure 3.4 (b) that at onset of dryout at 3340 sec the temperature of the bed is rising rapidly due to the fact that as maximum heat removal rate is achieved hence it cannot remove any further amount of heat . Since heat is accumulating inside the bed there is an increase in bed temperature. Figure 3.4 (c) shows steady increase of vapour mass with advancing time as more amount of water vapour is formed from the liquid state with increase in heat.

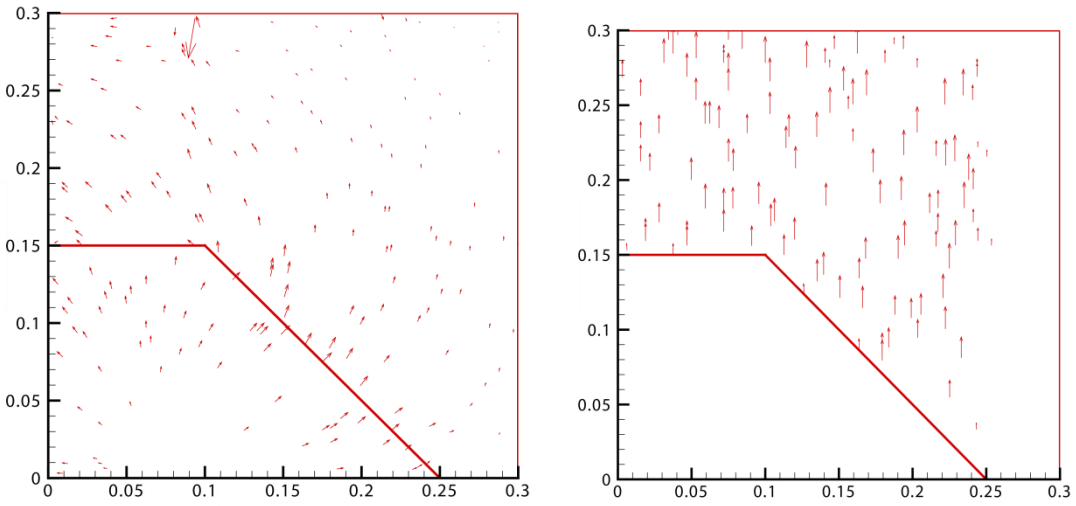

(a) **(b)**

Figure 3.5 Velocity vectors of (a) Water (b) Vapour

Inside the enclosure due to rise in temperature of the water and vapour inside the bed a temperature gradient is formed which will cause a buoyancy related motion from the bed. The figure 3.5 shows the direction of velocity vectors of the fluids occurring from the bed.

Case 2 When simulation was conducted at 2 bar pressure for 3600 seconds

For the given 2 bar pressure the initial temperature of top wall, left wall, water and the debris are maintained at saturation temperature of 393.36 K. After a series of trial it was found that the minimum dryout power for 2 bar pressure for a run time of 3600 seconds is 16 kW. It is to be noted that with increase in pressure there is an increase in dryout power this is due to the fact that with higher operating pressure there will be increase in vapour density which will occupy lesser space for the same mass transfer rate. Hence in order to accumulate vapour at the bed more mass transfer is required which can be ensured by increasing the heating power. At the time duration of 3060 seconds dryout phenomenon was observed. Dryout was marked with vapour accumulation at the top of the bed and a steep rise in solid temperature.

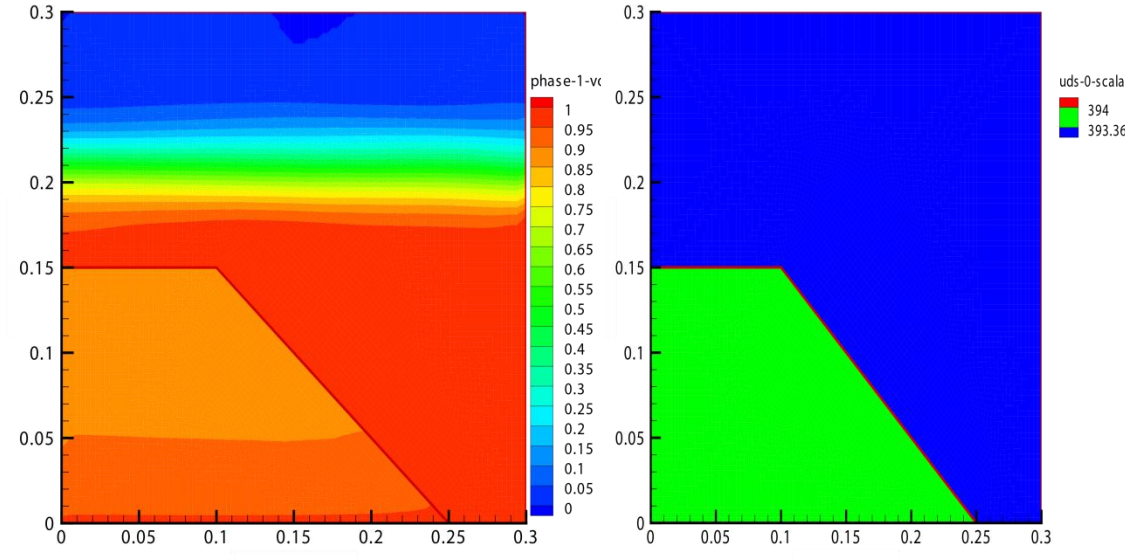

(a) **(b)**

Figure 3.6 (a) No vapour accumulation in the debris bed at 2000 sec; (b) Bed temperature at 2000 sec.

Heat generation inside the solid results in increase in temperature of the debris bed. The heat is transferred to the surrounding liquid due to convection as a result temperature of the liquid starts to rise. Once the liquid temperature reaches the saturation temperature it starts to boil and results in formation of vapour. Heat transfer starts to take place between solid to vapour and from vapour to liquid. In the above figure 3.6 we can see that although vapour is starting to form inside the bed the temperature of the bed lies very close to saturation temperature. Thus it implies that as the heat from the bed is removed sufficiently the temperature of the bed is not rising.

It is clearly seen from the above figure 3.6 that dryout was not achieved at 2000 seconds because there is no vapour accumulating inside the bed.

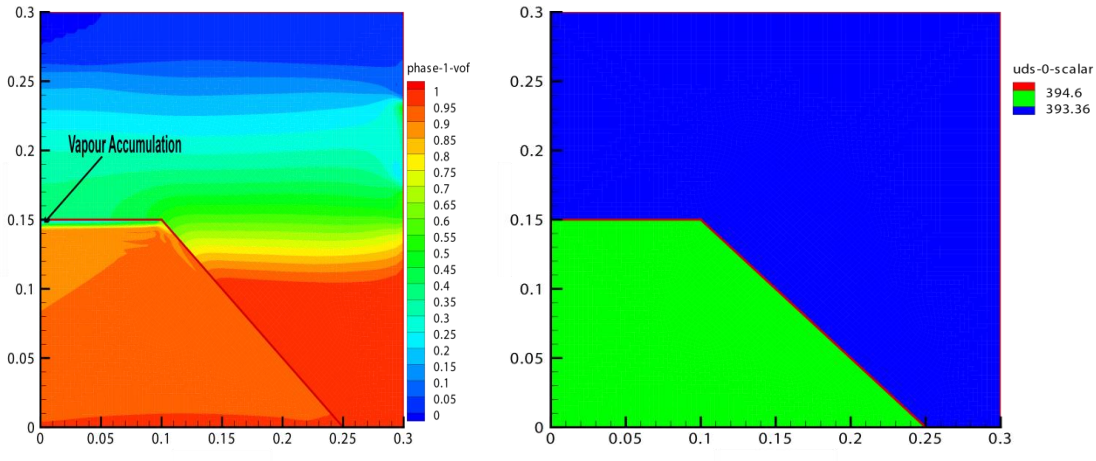

Figure 3.7 (a) Development of dryout in the debris bed at 3060 sec in terms of liquid saturation and (b) bed temperature at 3060 sec.

This heat removal process continues until a stage comes when it reaches a limit beyond which the debris cannot be maintained in a coolable state. This is known as dryout condition. In the figure 3.7 we can see that dryout point has been attained and since heat is accumulating inside the bed the temperature of the bed is rising.

We can clearly see from the above figure 3.7 that at the onset of dryout vapour is just starting to accumulate at the top of the bed with a slight increase in temperature of the bed also occurring.

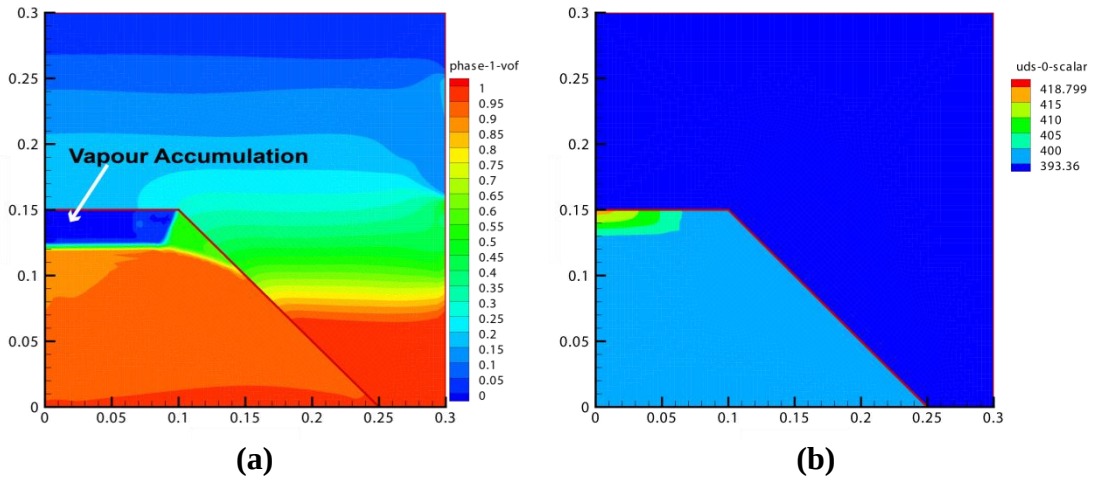

Figure 3.8 (a) Vapour accumulation at the top of the debris bed at the end of 3600 seconds (b) Bed temperature at the end of 3600 seconds.

From Figure 3.8 we can see that after a significant time has elapsed since dryout, vapour formation is building up at the debris bed and there has been a steep rise in temperature of the bed due to accumulation of the heat.

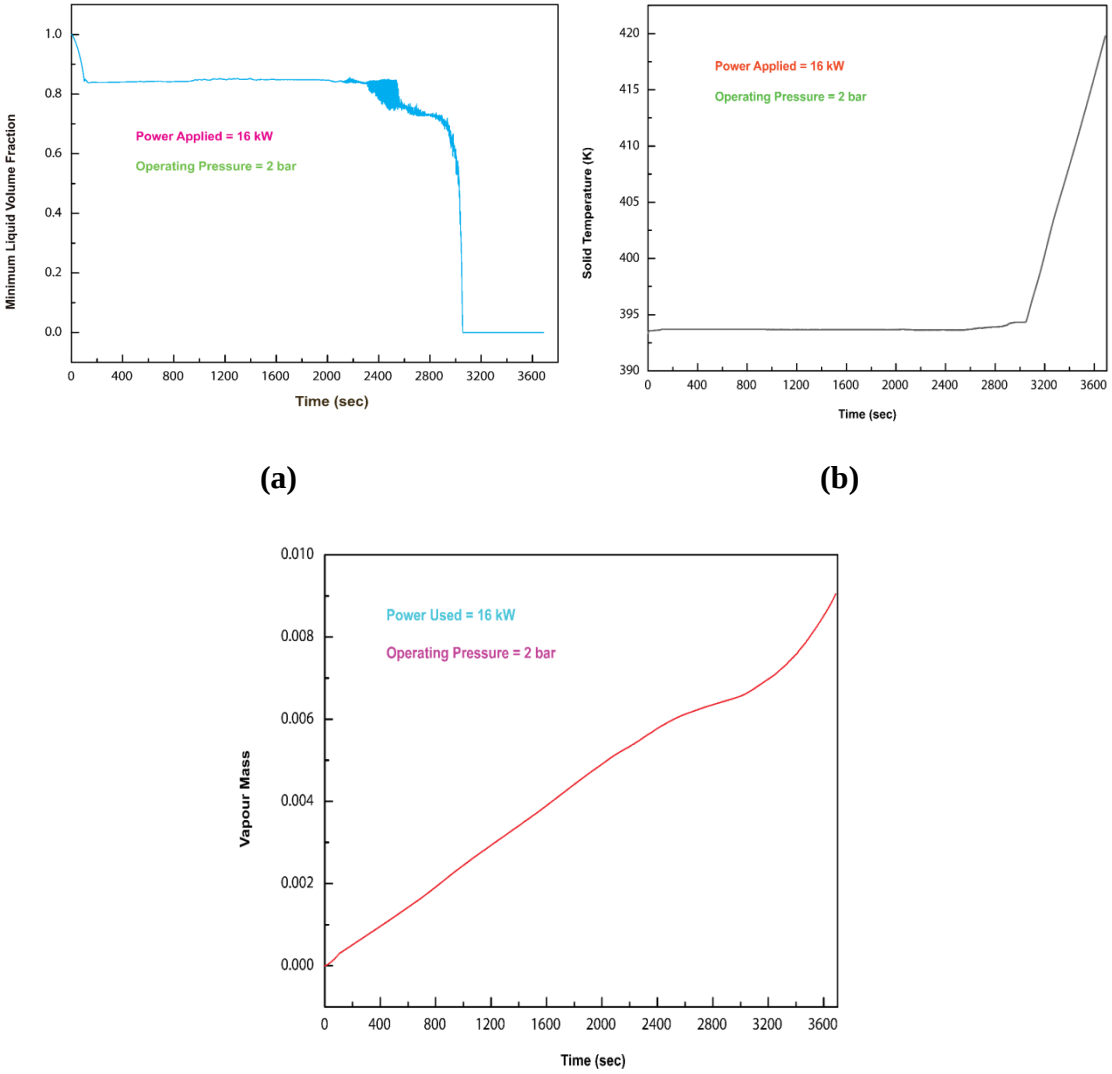

Figure 3.9 (a) shows minimum liquid volume fraction versus time inside the debris bed (b) shows maximum solid temperature versus time inside the debris bed (c) shows vapour mass generated versus time inside the debris bed

Figure 3.9 (b) indicates the rise of bed temperature after attaining the dryout at 3060 seconds.

Figure 3.9 (c) shows steady increase of vapour mass with advancing time as more amount of water vapour is formed from the liquid state with increase in heat.

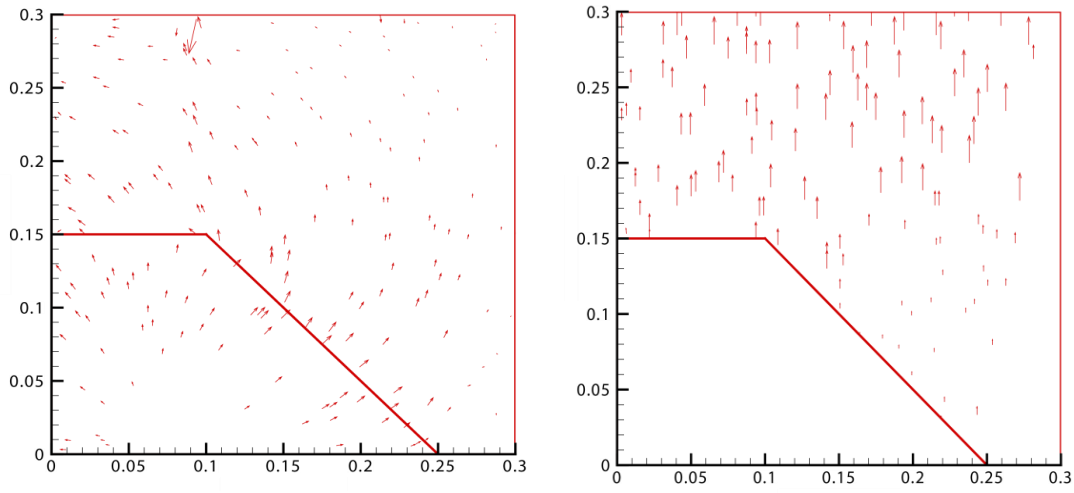

(a) **(b)**

Figure 3.10 Velocity vectors of (a) Water (b) Vapour

Inside the enclosure due to rise in temperature of the water and vapour inside the bed a temperature gradient is formed which will cause a buoyancy related motion from the bed. The figure 3.10 shows the direction of velocity vectors of the fluids occurring from the bed.

Case 3 When simulation was conducted at 1 bar pressure for 3600 seconds at various wall temperatures

In this given case simulations were conducted for various subcooled conditions like 1K, 2K, 4K, 6K and 8K. The simulations were each conducted for 1 bar pressure for a run time of 3600 seconds. The heating power applied for each cases as discussed below is 15 kW. The following conditions are to be noted down:

(a) For all the cases the temperature of the debris was kept at the saturated temperature of 372.7559 K.
(b) For 1K condition the initial temperatures of water and the top and the left walls of the enclosure are kept at 371.7559 K.
(c) For 2K condition the initial temperatures of water and the top and the left walls of the enclosure are kept at 370.7559 K.
(d) For 4K condition the initial temperatures of water and the top and the left walls of the enclosure are kept at 368.7559 K.
(e) For 6K condition the initial temperatures of water and the top and the left walls of the enclosure are kept at 366.7559 K.
(f) For 8K condition the initial temperatures of water and the top and the left walls of the enclosure are kept at 364.7559 K.

As per the conditions, the required values are also changed according to the temperatures.

For all the above simulations conducted dryout was not achieved at the end of the stipulated run time.

The figure 3.11 indicates liquid volume fraction for all the cases at the end of 3600 seconds.

We can observe from the above figure that with increase in liquid subcooling the volume of fraction of liquid increases. This is due to the fact that with increase in subcooling heat transfer from the debris is increased as a result the coolability of the enclosure is also increased. When subcooled condition is applied there will be a delay in the boiling of water and with increase in liquid subcooling the time interval till the onset of boiling will become longer. When boiling commences it results in formation of vapour which when comes in contact with cooled liquid condenses back to liquid form again. With increase in subcooling more amount of vapour formed will be condensed back to liquid. This will ensure more heat removal from the debris and will confine the vapour into a small region inside the debris bed.

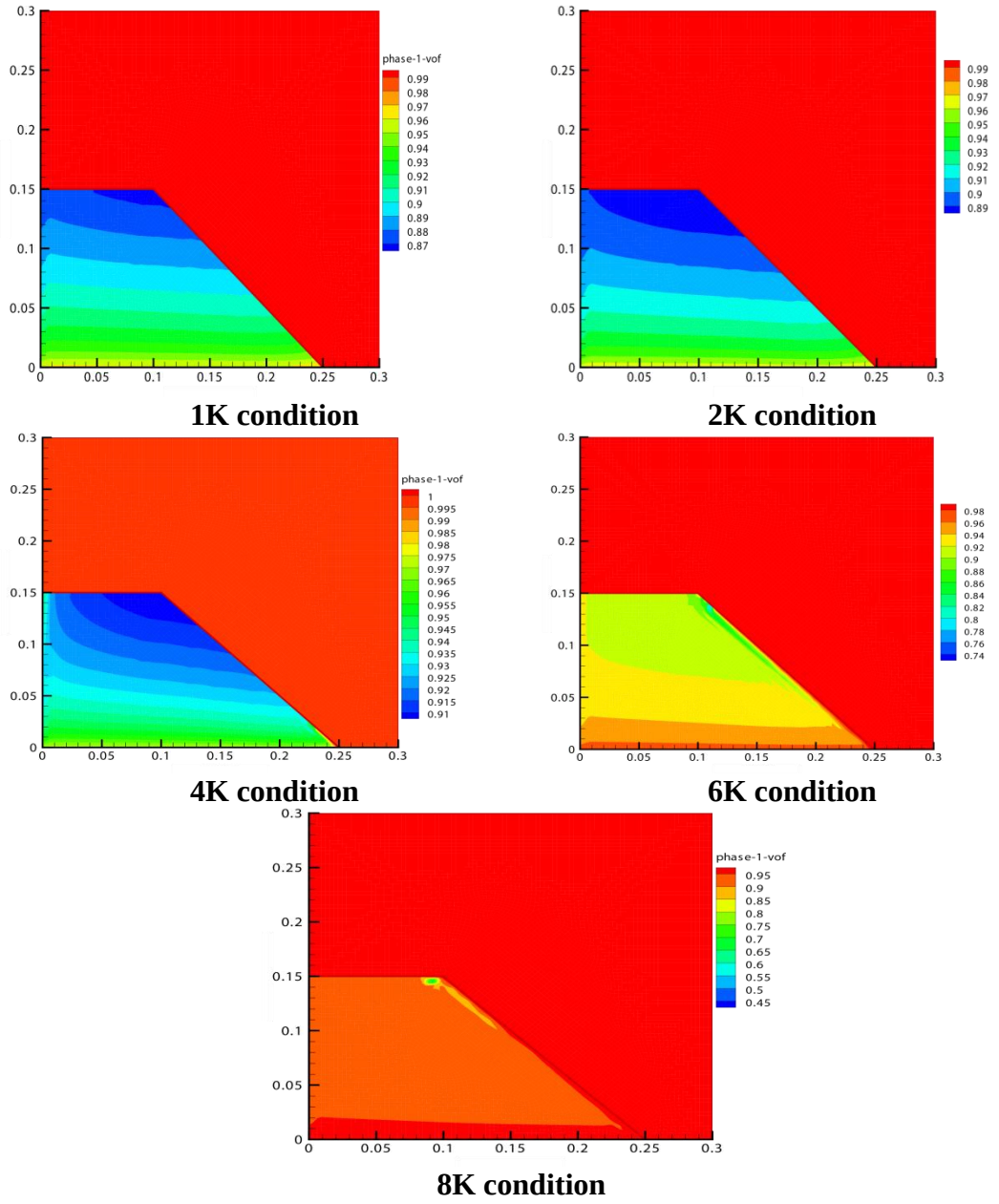

Figure 3.11 shows liquid volume fraction after 3600 seconds for all the various wall variation conditions. The heating power applied for each case is 15kW.

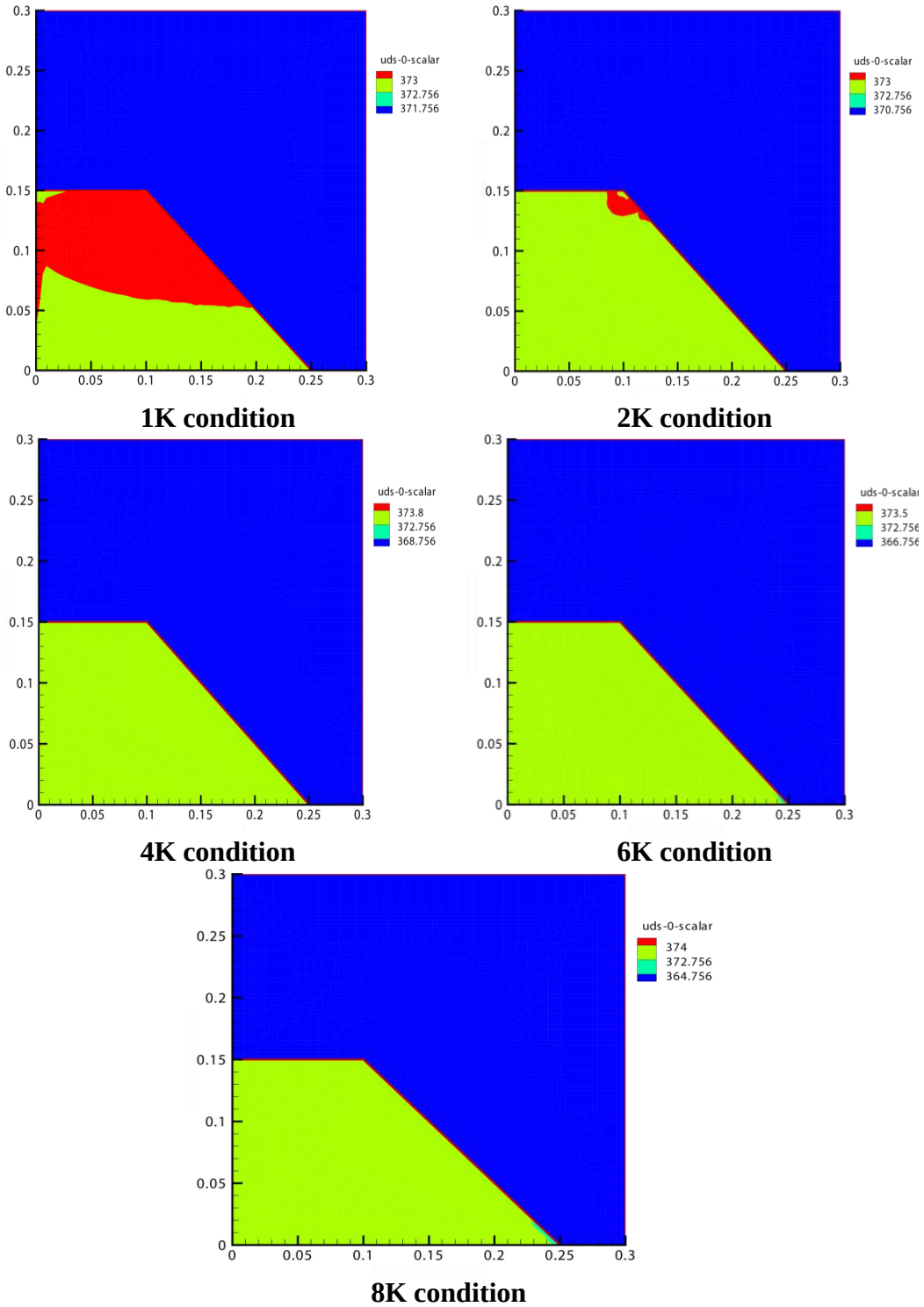

Figure 3.12 The above figures show the temperature of the debris bed after 3600 seconds for various wall variation temperature. The heating power applied for each case is 15 kW.

Thus we can conclude that with increase in wall variation temperature the heat transfer rate at the top and left walls are increasing due to increase in convection. This can be detected from the above figures that with increase in subcooling

temperature the liquid penetration in the heated bed is increased and more amount of heat is taken away by the liquid thus keeping the bed in a relatively cooled state.

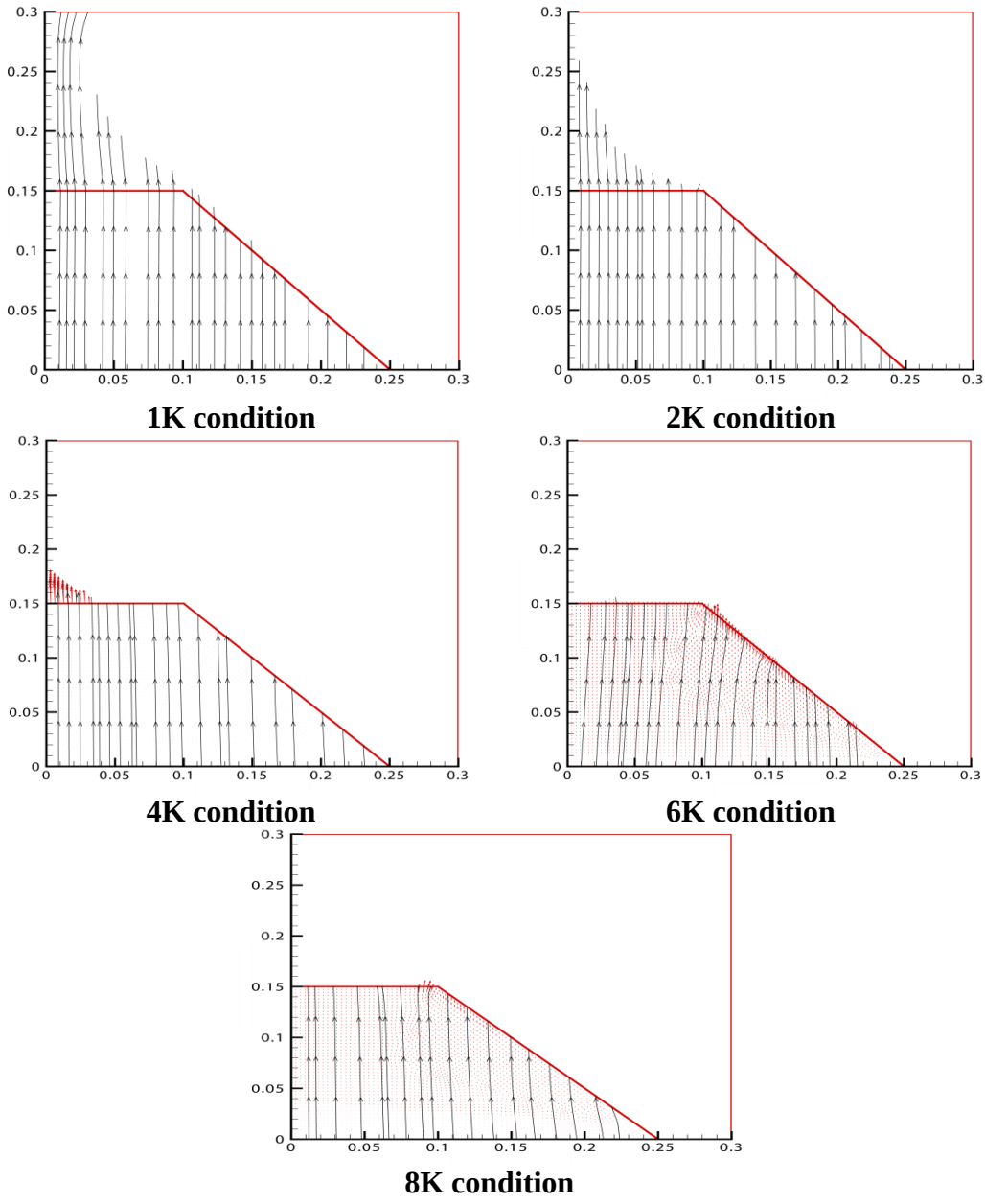

Figure 3.13 The above figures show vapour steam traces after 3600 seconds for all the various wall variation conditions at the heating power of 15 kW.

From the figure 3.13 we can clearly see that with increase in wall subcooling temperatures better coolability of the debris bed is ensured as more amount of heat is taken away from the bed which is resulting in formation of lesser amount of vapour emerging from the bed.

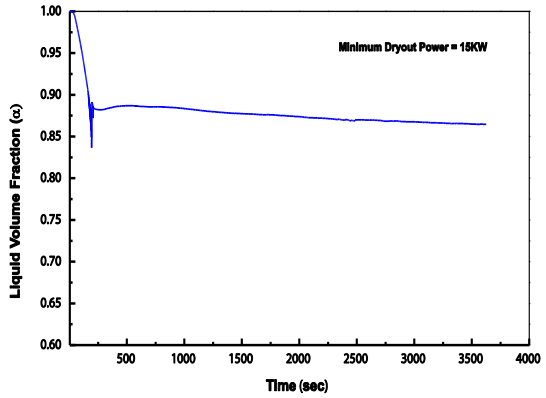

1K subcooling

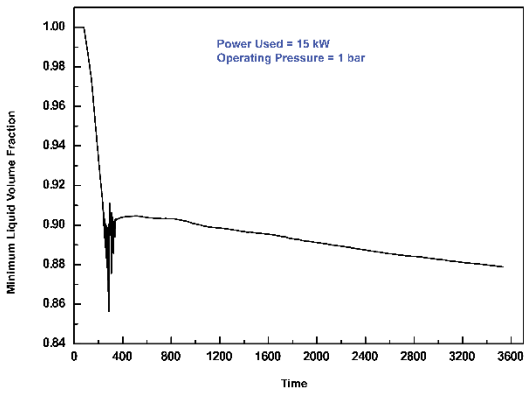

2K subcooling

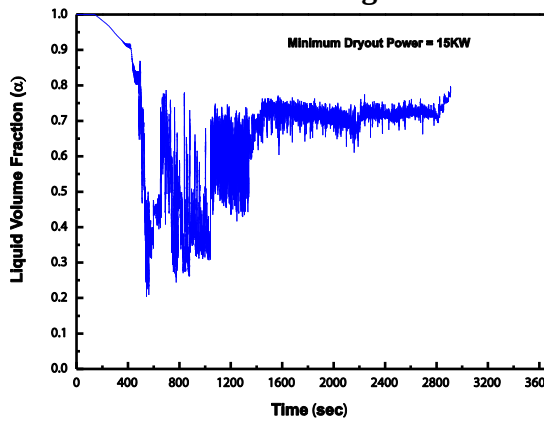

4K subcooling

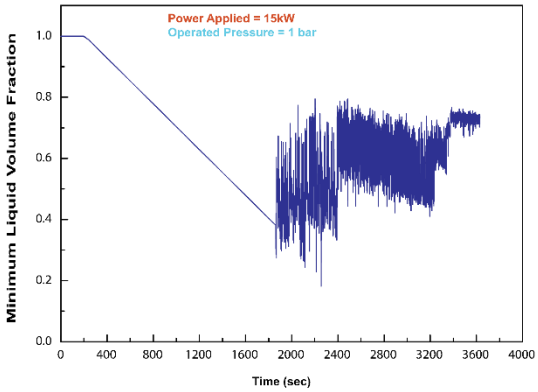

6K subcooling

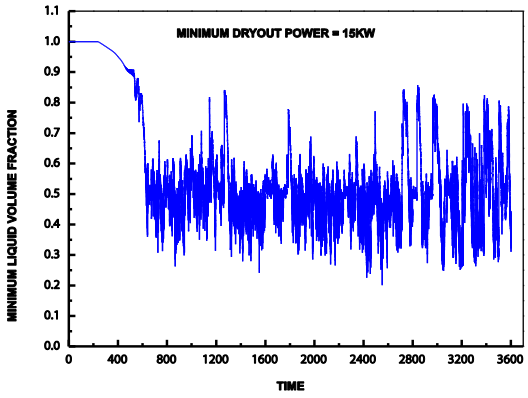

Figure 3.14 shows the minimum liquid volume fraction inside the bed versus time for various subcooling cases.

It is evident from the above graphs of figure 3.14 that dryout was not achieved in any cases discussed above.

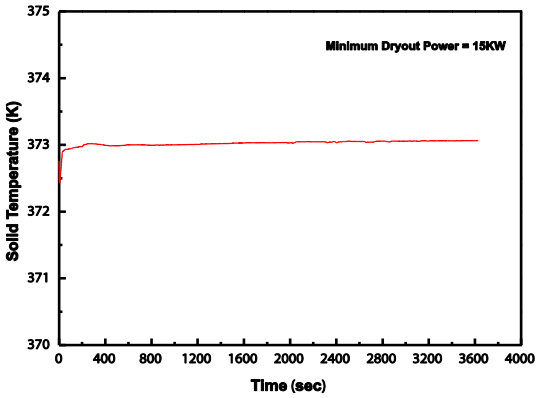

1K subcooling

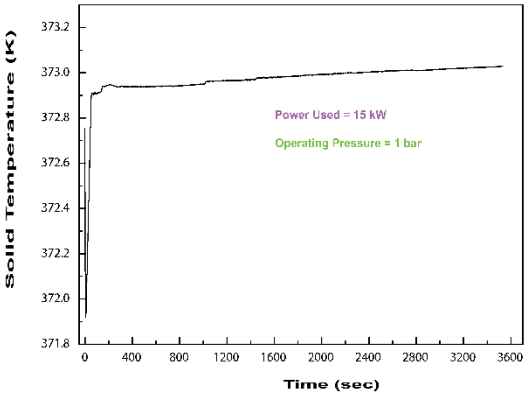

2K subcooling

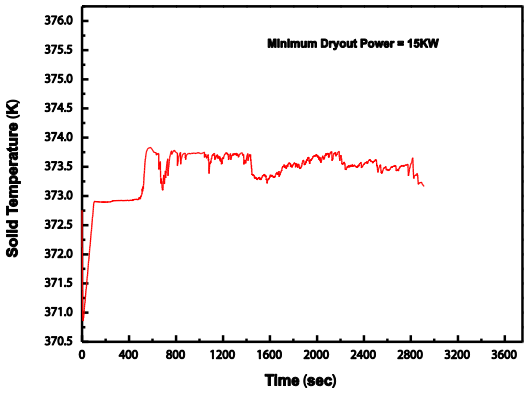

4K subcooling

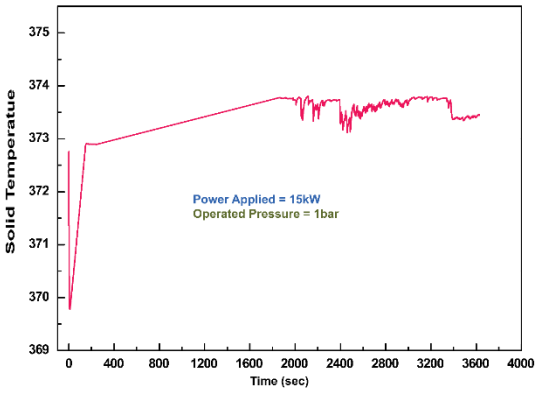

6K subcooling

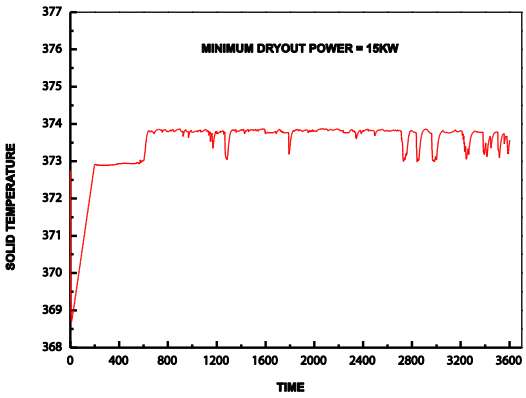

8K subcooling

Figure 3.15 shows the maximum solid temperature inside the bed versus time for various subcooling cases.

It is clearly seen from the above graphs at figure 3.15 that due to better coolability of the enclosure the maximum solid temperature is not rising and is more or less holding constant with time.

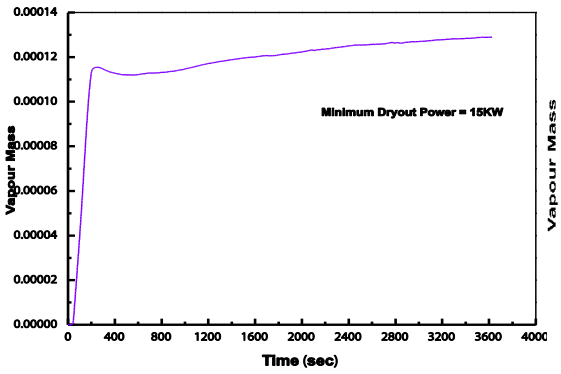

1K subcooling

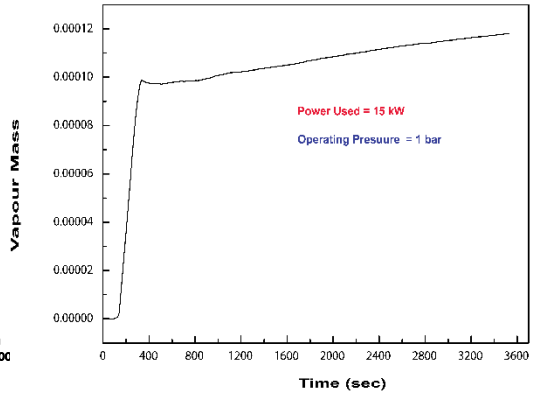

2K subcooling

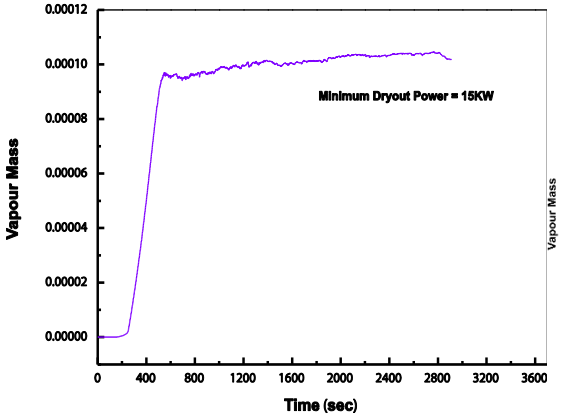

4K subcooling

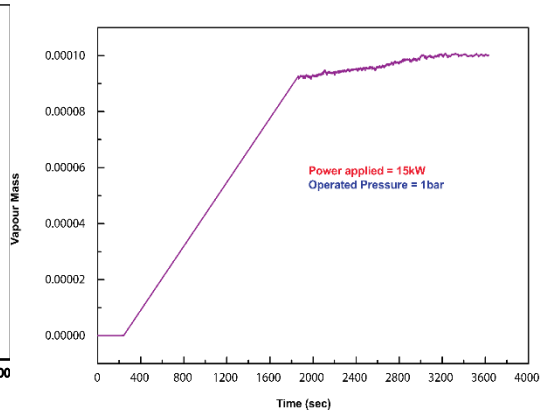

6K subcooling

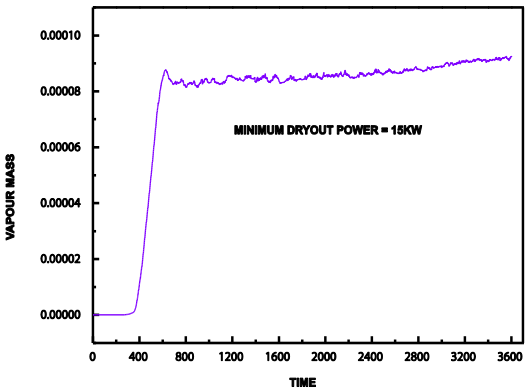

8K subcooling

Figure 3.16 shows the vapour mass versus time for various subcooling cases.

We can clearly see that with increase in wall subcooling temperatures there is an increase in amount of heat flux out of the enclosure from the left wall with advancing time. This is ensuring better coolability of the debris bed.

Case 4 When simulation was conducted at 1 bar pressure for 3600 seconds at 1K variation of wall temperatures

For the given 1 bar pressure the initial temperature of water, top wall and left wall was maintained at 371.7559 K but the debris are maintained at saturation temperature of 372.7559 K. After a series of trial it was found that the minimum dryout power for 1 bar pressure at 1K variation in temperature for a run time of 3600 seconds is 24 kW. At the time duration of 2880 seconds dryout phenomenon was observed. Dryout was marked with vapour accumulation at the top of the bed and a steep rise in solid temperature.

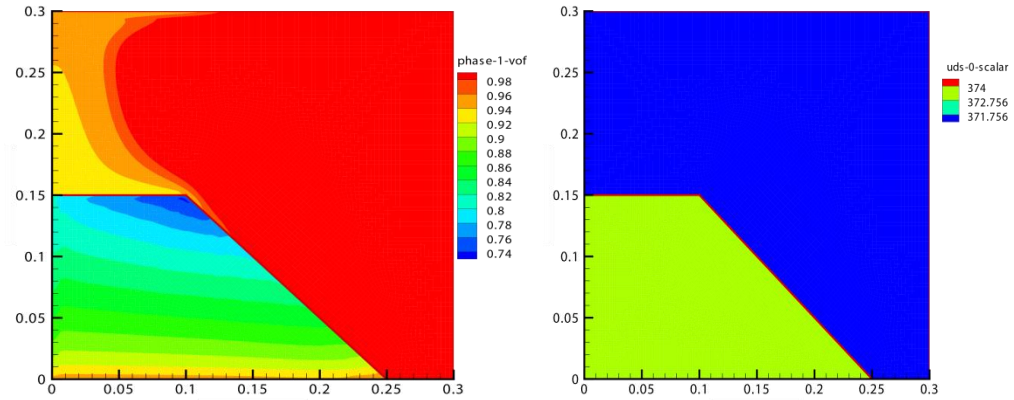

(a) **(b)**

Figure 3.17 (a) shows liquid volume fraction at the end of 2000 seconds.

(b) shows bed temperature at the end of 2000 seconds.

Heat generation inside the solid results in increase in temperature of the debris bed. The heat is transferred to the surrounding liquid due to convection as a result temperature of the liquid starts to rise. Once the liquid temperature reaches the saturation temperature it starts to boil and results in formation of vapour. Heat transfer starts to take place between solid to vapour and from vapour to liquid. In the above figure we can see that although vapour is starting to form inside the bed the temperature of the bed lies very close to saturation temperature. Thus it implies that as the heat from the bed is removed sufficiently the temperature of the bed is not rising.

It is clearly visible from the above figure 3.17 that dryout was not achieved at 2000 seconds because there is no vapour accumulating inside the bed.

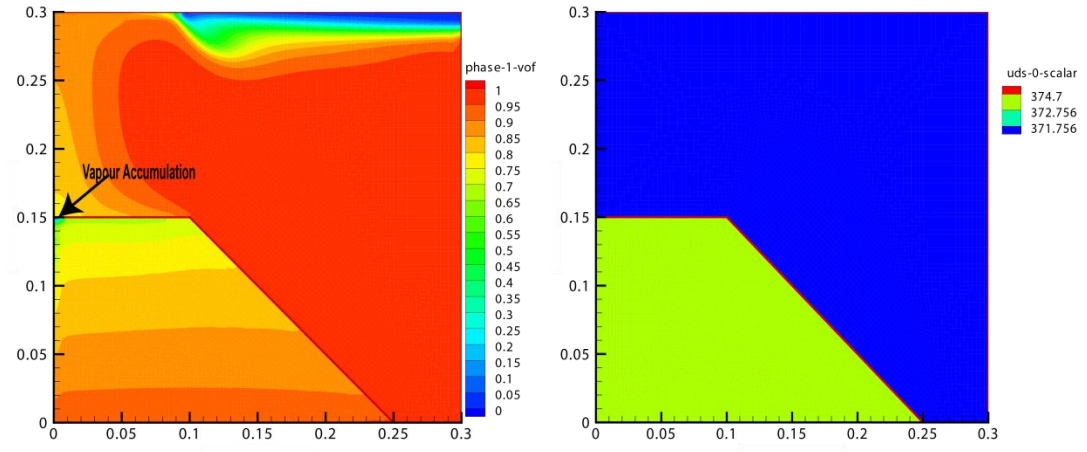

(a) **(b)**

Figure 3.18 (a) shows liquid volume fraction at the end of 2880 seconds.

(b) shows bed temperature at the end of 2880 seconds.

This heat removal process continues until a stage comes when it reaches a limit beyond which the debris cannot be maintained in a coolable state. This is known as dryout condition. In the figure we can see that dryout point has been attained and since heat is accumulating inside the bed the temperature of the bed is rising.

We can clearly see from the above figure that at the onset of dryout vapour is just starting to accumulate at the top of the bed with a slight increase in temperature of the bed also occurring.

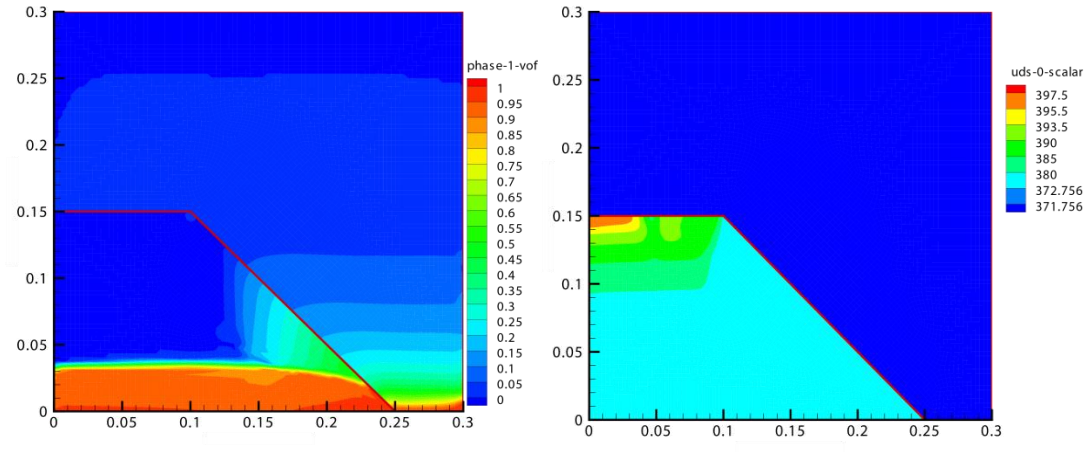

(a) **(b)**

Figure 3.19 (a) shows liquid volume fraction at the end of 3600 seconds. (b) shows bed temperature at the end of 3600 seconds.

The figure 3.19 above shows the condition of the bed after the dryout point has been attained when more than half of the bed volume is being covered by vapour. The figure 3.19 (b) shows the rise in temperature of the bed after 3600 seconds as further amount of heat energy cannot be removed as dryout point has been reached.

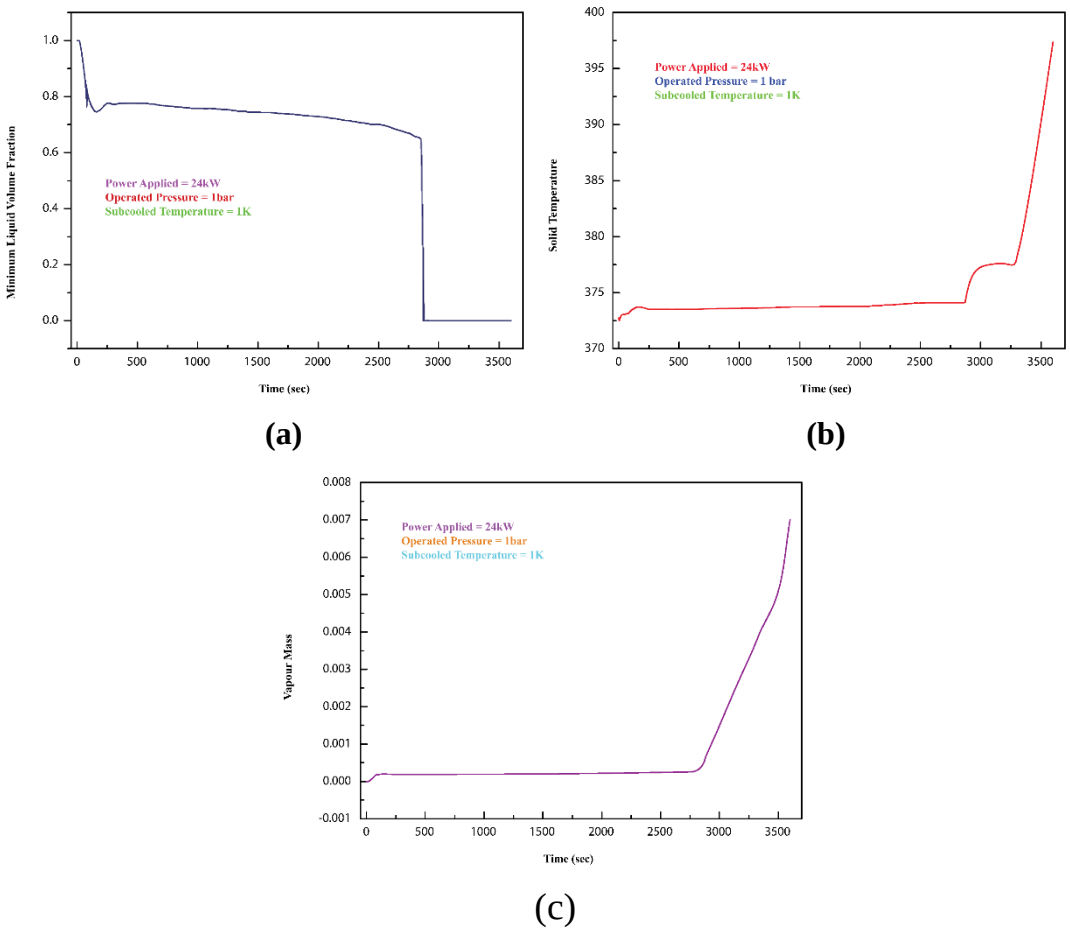

Figure 3.20 (a) Minimum liquid volume fraction of the bed versus time (b) Maximum solid temperature of the bed versus time (c) Vapour mass versus time

The above figures clearly indicate that after the dryout point has been achieved there is a steep rise in the bed temperature. Also there is an increase in vapour mass with time as more amount of liquid is getting converted into vapour.

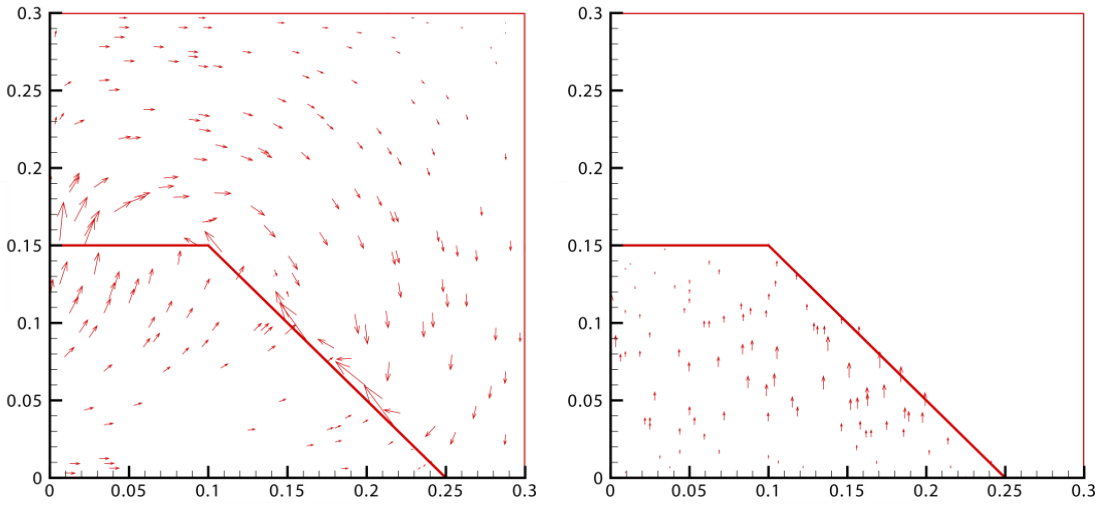

(a) **(b)**

Figure 3.21 Velocity vectors of (a) Water (b) Vapour

Inside the enclosure due to rise in temperature of the water and vapour inside the bed a temperature gradient is formed which will cause a buoyancy related motion from the bed. The figure shows the direction of velocity vectors of the fluids occurring from the bed

Case 5 When simulation was conducted at 1 bar pressure for 3600 seconds at 2K variation of wall temperatures

For the given 1 bar pressure the initial temperature of water, top wall and left wall was maintained at 370.7559 K but the debris are maintained at saturation temperature of 372.7559 K. After a series of trial it was found that the minimum dryout power for 1 bar pressure at 2K variation in temperature for a run time of 3600 seconds is 30 kW. At the time duration of 2710 seconds dryout phenomenon was observed. Dryout was marked with vapour accumulation at the top of the bed and a steep rise in solid temperature.

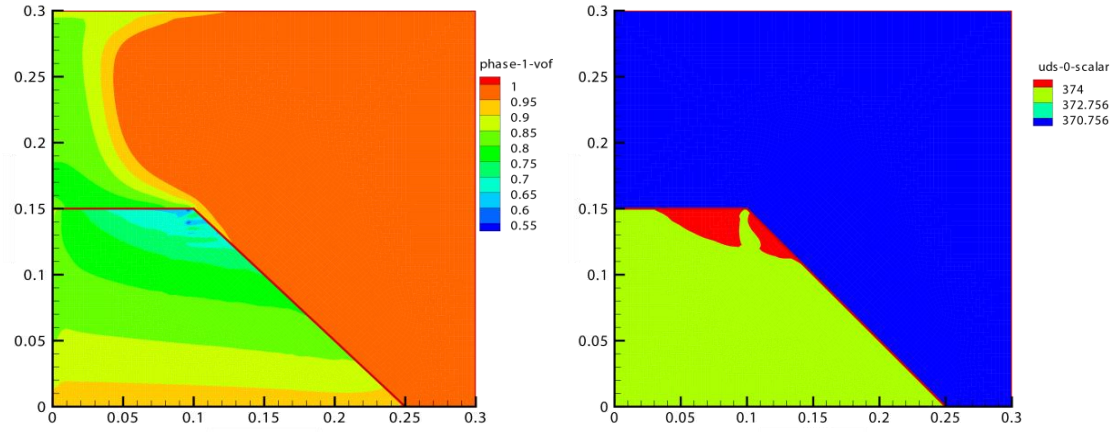

(a) **(b)**

Figure 3.22 (a) liquid volume fraction of the bed at 2000 seconds (b) temperature of the bed at 2000 seconds.

Heat generation inside the solid results in increase in temperature of the debris bed. The heat is transferred to the surrounding liquid due to convection as a result temperature of the liquid starts to rise. Once the liquid temperature reaches the saturation temperature it starts to boil and results in formation of vapour. Heat transfer starts to take place between solid to vapour and from vapour to liquid. In the above figure we can see that although vapour is starting to form inside the bed the temperature of the bed lies very close to saturation temperature. Thus it implies that as the heat from the bed is removed sufficiently the temperature of the bed is not rising.

It is clearly visible from the above figure 3.22 that dryout was not achieved at 2000 seconds because there is no vapour accumulating inside the bed.

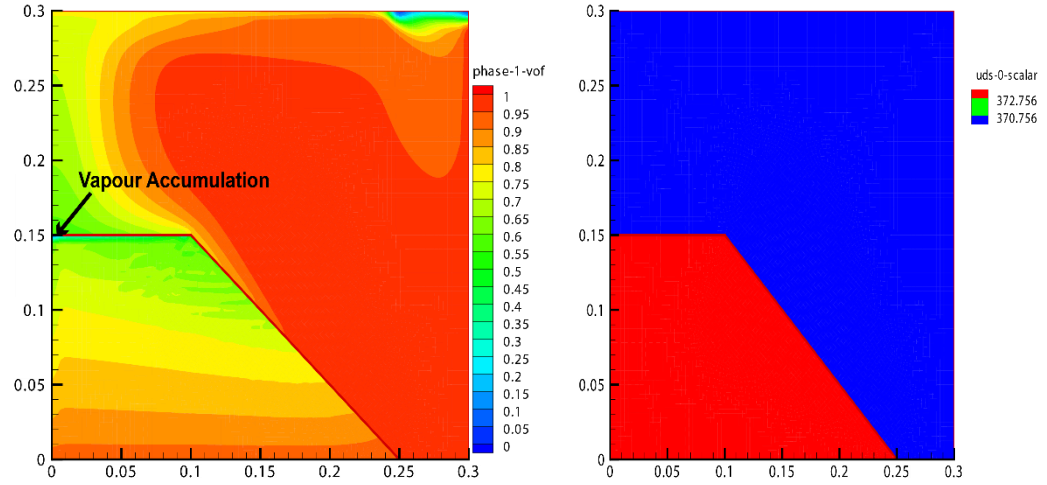

(a) **(b)**

Figure 3.23 (a) shows the liquid volume fraction of the bed at 2710 seconds.

(b) temperature of the debris bed at 2710 seconds.

This heat removal process continues until a stage comes when it reaches a limit beyond which the debris cannot be maintained in a coolable state. This is known as dryout condition. In the figure we can see that dryout point has been attained and since heat is accumulating inside the bed the temperature of the bed is rising.

The above figure 3.23 clearly shows that at the onset of dryout at 2710 seconds there is an accumulation of vapour at the top of the bed with temperature rising in that particular region. The rise in temperature of the bed is due to the fact that there is accumulation of heat energy as the maximum level of heat dissipation from the bed is reached.

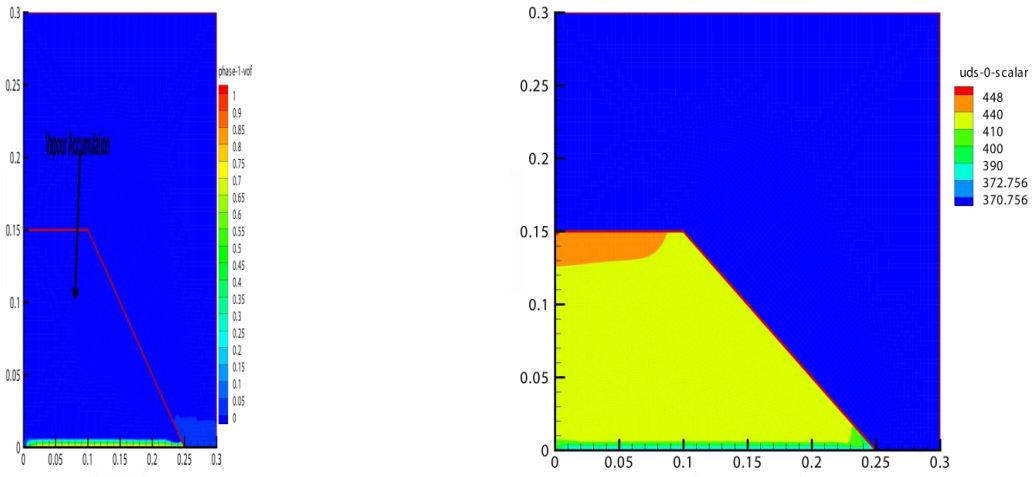

Figure 3.24 (a) liquid volume fraction of the bed at 3600 seconds. (b) temperature of the bed at the 3600 seconds.

The figure 3.24 above shows the condition of the bed after the dryout point has been attained when the entire bed is being covered by vapour at 3600 seconds. The figure 3.24 (b) shows the rise in temperature of the bed after 3600 seconds as further amount of heat energy cannot be removed as dryout point has been reached.

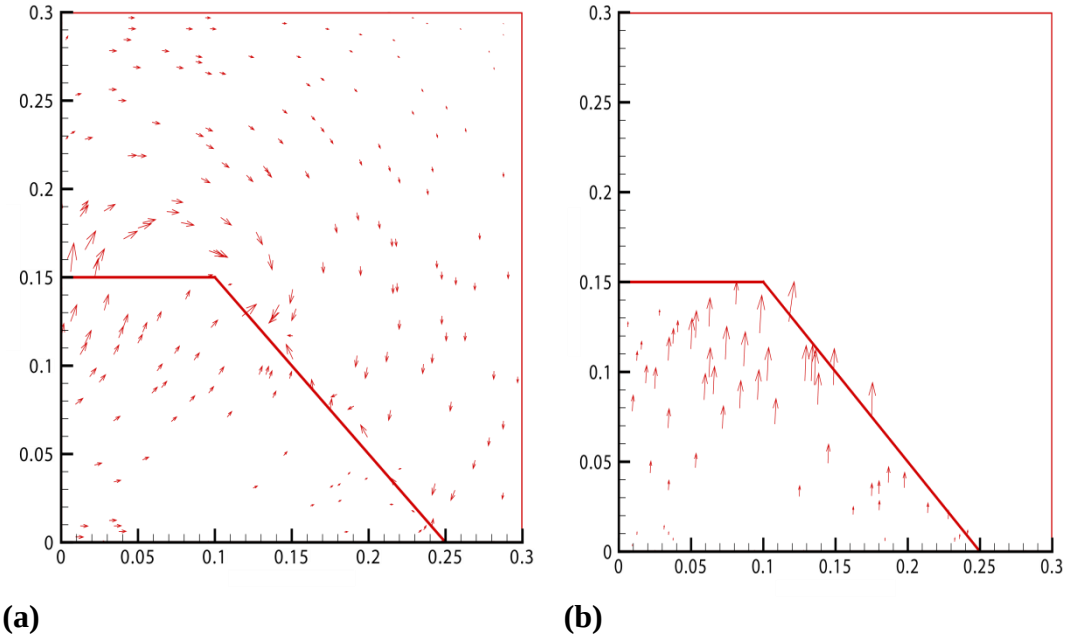

Figure 3.25 Velocity vectors of (a) Water (b) Vapour

Inside the enclosure due to rise in temperature of the water and vapour inside the bed a temperature gradient is formed which will cause a buoyancy related motion from the bed. The figure shows the direction of velocity vectors of the fluids occurring from the bed

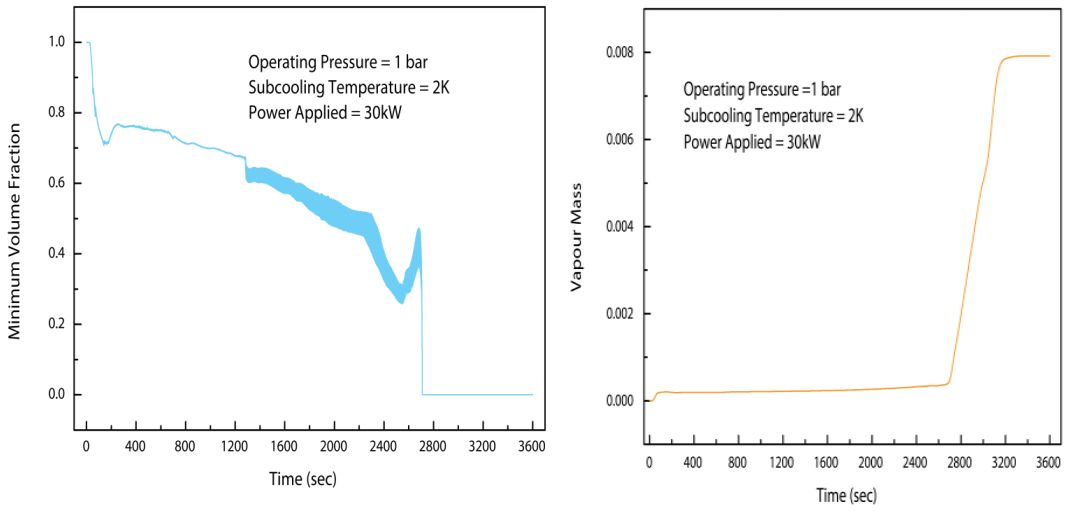

Figure 3.26 (a) shows minimum volume fraction of liquid versus time (b) vapour mass formation versus time

Chapter 4

CONCLUSION

4.1 SUMMARY OF THE WORK

Any kind of nuclear accident is very unfortunate incident and precautions have to be taken to avoid it at all cost. But in case if we face one, steps have to be taken to arrest the progression of the accident as quickly as possible. In case of a severe nuclear accident one of the key obstacles faced will the loss of electric power with the inevitable consequence of failure of core cooling system. At this point of time the biggest challenge will be to protect the core by cooling it down continuously. The present study showed that core cooling by natural convection is a very useful means to protect it from further degrading.

In the present study analysis has carried out for a heat generating truncated cone shaped debris by considering a multiphase flow situation. In this regard debris model is used within the framework of the commercial CFD platform ANSYS FLUENT with extensive use of user-defined functions. Simulations were conducted under different criteria to obtain results for the project which is being carried out.

From the results obtained by simulations it can be concluded that with increase in pressure the dryout power increases. It is observed from the present study that at 1 bar pressure the minimum dryout power obtained after 3600 seconds is 15kW which increases to 16kW when the simulation is carried at 2 bar pressure for the same stipulated time.

Another important observation from the present study of natural convection is that when the walls of the enclosure and the coolant are maintained at a particular subcooling below the saturation temperature dryout of a debris bed can be avoided for a given applied power as compared to a situation when subcooling of the walls and coolant are not maintained and dryout phenomenon is observed for the same power applied. Thus we can conclude that better coolability of the bed was attained in case of a situation when subcooling was maintained.

In the given context it is also observed that for a given scenario the minimum dryout power increases when subcooling for the coolant and wall enclosures are applied. For example for a runtime of 3600 seconds at 1 bar pressure the minimum dryout power obtained is 15kW when no subcooling is maintained. But when a subcooling of 1 K is maintained the minimum dryout power increases to 24kW. In case of 2 K subcooling, the minimum dryout power increases to 30kW for the same pressure and runtime. Thus it can be concluded with increase in subcooling minimum

dryout power increases thus better coolability of the bed can be ensured. Table 4.1 summarises about the effect of system pressure and degree of subcooling on the Dry-out power.

Table 4.1 Effect of system pressure and degree of subcooling on the Dryout power

System pressure (bar)	Degree of subcooling (K)	Dryout Power (kW)
1	0	15
	1	24
	2	30
2	0	16

4.2 SCOPE OF FUTURE WORK

For future studies an effort can be made to vary the dimensions of the debris bed by keeping the volume and the shape constant. Keeping this in mind study of natural convection using multiphase flow can be conducted.

Another point is that bed porosity is kept constant for the present study but in realistic situation the porosity is bound to vary. Studies can be conducted in future by changing the bed porosity which will align itself to a realistic kind of situation.

References

1. Bürger, M., Buck, M., Pohlner, G., Rahman, S., Kulenovic, R., Fichot, F., Ma, W., Miettinen, J., Lindholm, I., Atkhen, K.: *Coolability of particulate beds in severe accidents: Status and remaining uncertainties*. Prog. Nucl. Energ. **52**, 61-75 (2010).
2. Karbojian, A., Ma, W.M., Kudinov, P., Dinh, T.: *A scoping study of debris bed formation in the DEFOR test facility*. Nucl. Eng. Des. **239**, 1653-1659 (2009).
3. Lin, S., Cheng, S., Jiang, G., Pan, Z., Lin, H., Wang, S., Wang, l., Zhang, X., Wang, B.: *A two-dimensional experimental investigation on debris bed formation behaviour*. Prog. Nucl. En.**96**, 118-132 (2017).
4. Lindholm, I., Holmström, S., Miettinen, J., Lestinen, V., Hyvärinen, J., Pankakoski, P., Sjövall, H.: *Dryout heat flux experiments with deep heterogeneous particle bed*.Nucl. Eng. Des. **236,** 2060-2074 (2006).
5. Ma, W.M., Dinh, T.N.: *The effects of debris bed's prototypical characteristics on corium coolability in a LWR severe accident*. Nucl. Eng. Des.**240**, 598-608 (2010).
6. Magallon, D.: *Characteristics of corium debris bed generated in large-scale fuel-coolant interaction experiments*. Nucl. Eng. Des. **236**, 1998-2009 (2006).
7. Magallon, D., Huhtiniemi, I.: *Corium melt quenching tests at low pressure and subcooled water in FARO*. Nucl. Eng. Des.**204**, 369-376 (2001).
8. Miyazaki, K., Murai, K., Ohama, T., Yamaoka, N., Inoue, S.: *Pressure dependence of the particle bed dryout heat flux*. Nucl. Eng. Des.**95,** 271-273 (1986).
9. Reed, A.W., Bergernon, E.D., Boldt, K.R., Schmidt, T.R.: *Coolability of UO2 debris beds in pressurized water pools: DCC-1 and DCC-2 experiment results*. Nucl. Eng. Des. **97**(1), 81-88 (1986).
10. Schäfer, P., Groll, M., Kulenovic, R.: *Basic investigations on debris cooling*. Nucl. Eng. Des. **236**, 2104-2116 (2006).

11. Squarer, D., Pieczynski, A.T., Hochreiter, L.E.: *Effect of debris bed pressure, particle size and distribution on degraded nuclear reactor core coolability*. Nucl. Sci. Eng. **80**(1), 2-13 (1982).

12. Takasuo, E.: *An experimental study of the coolability of debris beds with geometry variations.Ann. Nucl. Energy* **92**, 251-261(2016).

13. Wang, C.H., Dhir, V.K.: *An experimental investigation of multidimensional quenching of a simulated core debris bed*. Nucl. Eng. Des.**110,** 61-72 (1988).

14. Yakush, S., Kudinov, P., Dinh, T.N.: *Modeling of two-phase natural convection flows in a water pool with a decay-heated debris bed*. Proceedings of ICAPP '08, California, USA (2008).

15. P.P.Kulkarni, M.R., R. Kulenovic, A.K.Nayak,*Experimental Investigation of Coolability Behaviour of Irregularly Shaped Particulate Debris Bed*. Nucl. Eng. Des. **240**, 3067-3077 (2010).

16. Chakravarty A, Datta P, Ghosh K, Sen S, Mukhopadhyay A, 2017 "*Natural Convective Heat Removal From A Heat Generating Corium Debris Bed*". Proc. 24th and 2nd International ISHMT-ASTFE Heat Mass Conference, BITS Pilani, Hyderabad, India, Paper No. IHMTC2017-11-0131,December 28-30 (2017).

17. Chakravarty,A.:*Numerical Modelling and Analysis of Debris Coolability using Porous Media Approach*. PhD Thesis, Jadavpur University, India (2018)

18. Jong K.Lee, SeungD.Lee and KuneY.Suh "*Natural Convection Heat Transfer In a Rectangular Water Pool With Internal Heating and Top and Bottom Cooling. Proceedings of ICONE14,International Conference On Nuclear Engineering, July 17-20,Miami,Florida,USA* (2006)

19. Seung Dong Lee and KuneYull Suh *Natural Convection Heat Transfer In Two-Dimensional Semicircular Slice Pool.* J. Nucl. Sci. Technol.,**40**,775-782 (2003).

20. Eunho Kim, Mooneon Lee, Hyun Sun Park, Kiyofumi Moriyama, Jin Ho Park *Development Of An Ex-Vessel Corium Debris Bed With Two-Phase Natural Convection In A Flooded Cavity.* Nucl. Eng. Des. **298**, 240-254 (2016).